

EXPOSURE TO HEAVY METAL STRESS REGULATES INTERCELLULAR SIGNALING
VIA CALLOSE DEPOSITION AND BREAKDOWN

Ruthsabel O'Levy

A DISSERTATION

in

Biology

Presented to the Faculties of the University of Pennsylvania

in

Partial Fulfillment of the Requirements for the

Degree of Doctor of Philosophy

2017

Supervisor of Dissertation

Kimberly L. Gallagher

Associate Professor of Biology

Graduate Group Chairperson

Michael Lampson, Ph.D., Associate Professor of Biology

Professor of Biology

Dissertation Committee

Doris Wagner (chair), Ph.D., Professor of Biology

Scott Poethig, Ph.D., Professor of Biology

Brian Gregory, Ph.D., Associate Professor of Biology

Jung-Youn Lee, Ph.D., Professor of Plant and Soil Sciences

EXPOSURE TO HEAVY METAL STRESS REGULATES INTERCELLULAR SIGNALING
VIA CALLOSE DEPOSITION AND BREAKDOWN

COPYRIGHT

2017

Ruthsabel O'Lexy

This work is licensed under the
Creative Commons Attribution-
NonCommercial-ShareAlike 3.0
License

To view a copy of this license, visit

<https://creativecommons.org/licenses/by-nc-sa/3.0/us/>

DEDICATION

To Douglas Prasher.

ACKNOWLEDGMENTS

I would like to thank my advisor, Dr. Kimberly Gallagher, for her support and generosity throughout my PhD. I treasure the trust she put in me, and the space she allowed me to become my own scientist. She has always backed my interests, whatever they have been. As her first graduate student, we have learned a lot together and I am grateful for the time I have spent developing here. That she is as excited as I am about the next step in my career speaks to how much she considers my success, her success.

My thesis committee: Dr. Doris Wagner, Dr. Scott Poethig, Dr. Brian Gregory, and Dr. Jung-Youn Lee, have been invaluable in the completion of this project. I cherish not only our formal annual meetings, but the opportunity to walk across the hall and exchange ideas and get guidance from scientists I truly respect and admire. I am honored to have worked with them and glad that they have always been on my side.

My collaborators Dr. Toru Fujiwara, Koji Kasai, Dr. Rosangela Sozzani, and Natalie Clark were kind enough to lend their expertise and teach me new skills that allowed for the completion of this work. I'd like to thank them for their hospitality and their shared excitement in my project; this would be a poorer story without their input.

My lab mates and the Plant Group have been a constant source of support and friendship that have made my time here rewarding and exciting. You have been a sort of 'supplemental' committee to me, and I have benefited from our brainstorming sessions and tutorials on things I needed help with. You have been great colleagues and associates.

Finally, I would like to thank my family. My parents and sisters have always been my biggest cheerleaders, and their unwavering pride and support have motivated me during many moments in this process. My husband, Tim, has been my partner and best friend long before I began this journey, and without his fiery support and eternal patience, this would not have been possible. It is hard to express how much his encouragement during times of bleakness meant to me and pushed me to keep going.

ABSTRACT

EXPOSURE TO HEAVY METAL STRESS REGULATES INTERCELLULAR SIGNALING VIA CALLOSE DEPOSITION AND BREAKDOWN

Ruthsabel O'Lexy

Kimberly Gallagher

How organisms sense external cues and integrate them into developmental changes remains a large biological question. Plants, which are sessile organisms, are particularly vulnerable to challenges in their environment. An early response to abiotic and biotic stress in plants is the modification of intercellular signaling through plasmodesmata, cytoplasmic channels that connect adjacent cells. However, the different ways in which plasmodesmata-mediated signaling can be affected, the molecular players involved in this response, the genetic basis of this regulation, and the biological benefits of this response are still poorly understood.

Here, we take a survey of seven different agriculturally relevant stresses of nutrient starvation and heavy metal contamination, and their effects on plasmodesmata transport in the *A. thaliana* root. We examine the role of the polysaccharide callose, a known plasmodesmata regulator, in these modifications. Focusing on the conditions of excess iron and copper, we take a genetic approach to identify the genes involved in callose metabolism under these conditions. Finally, we examine how modifications in plasmodesmata transport under stress affect plant growth, health, and tolerance to heavy metal stress.

We find that plasmodesmata closure in response to stress is not a universal response, as was previously believed. While most conditions do induce plasmodesmata closure, some heavy metals increase plasmodesmata permeability instead. In many of the conditions tested, the changes in plasmodesmata modification correlate with changes in callose deposition as expected. In further examining excess copper and iron stresses, we identify genes in the callose synthase and β -1,3-glucanase families that synthesize and breakdown callose, responsible for callose metabolism under these conditions. We observe that these regulated changes in

plasmodesmata signaling in response to stress affect root growth, health, and mineral distribution. Most importantly, opening plasmodesmata under excess copper allows for better root growth, improved tolerance to copper, and reduced copper levels in the root meristem.

TABLE OF CONTENTS

ACKNOWLEDGMENTS	IV
ABSTRACT.....	V
LIST OF TABLES	IX
LIST OF ILLUSTRATIONS	X
1. INTRODUCTION	1
Metal contamination of soils.....	3
Plant uptake of metals	4
Long-distance transport of metals.....	7
Root responses to metal excess	9
Metal accumulation in plants.....	10
Plasmodesmata structure	11
Movement of non-cell-autonomous factors in development.....	13
Plasmodesmata roles in biotic stress.....	16
Plasmodesmata roles in abiotic stress.....	16
Regulation of plasmodesmata signaling	19
2. RESULTS.....	25
Plasmodesmata-mediated transport is modified under conditions of nutrient stress.....	26
Changes in the accumulation of callose drive the response of the root to iron and copper	31
Callose synthases and β-1,3-glucanases control the levels of callose in response to excess iron and copper	34
Modifying plasmodesmatal permeability in response to iron or copper stress has consequences for plant growth.....	40

The distribution of copper is altered in the β -1,3-glucanase mutants	46
3. CONCLUSIONS AND FUTURE DIRECTIONS.....	50
Symplastic isolation of the phloem in response to iron stress	51
Increasing plasmodesmatal permeability in response to copper stress	53
The role of CalS and β -1,3-glucanase enzymes in responding to specific environmental cues	55
The link between callose deposition and primary root growth.....	56
Determining the mechanism of plasmodesma regulation under zinc stress	58
The role of ROS in heavy metal stress	60
4. MATERIALS AND METHODS	64
Plant material and growth conditions.....	65
Germplasm used in this study.....	66
Primers used in this study	67
Growth measurements	69
Aniline blue staining	69
GUS staining.....	69
CFDA transport assays	69
SUC2:GFP diffusion measurements	70
Raster Image Correlation Spectroscopy (RICS)	70
Laser Ablation – Inductively Coupled Plasma – Mass Spectroscopy (LA-ICP-MS).....	71
BIBLIOGRAPHY.....	72

LIST OF TABLES

Table 4.1 Germplasm used in this study.....	66
Table 4.2 Primers used in this study.....	67

LIST OF ILLUSTRATIONS

Figure 1.1 Mechanisms of metal accumulation in plants.....	6
Figure 1.2 General model of radial transport of heavy metals in the root	8
Figure 1.3 Routes of plasmodesmata transport.....	12
Figure 1.4 Mechanisms of plasmodesmata regulation.....	20
Figure 2.1 Changes in CFDA transport after heavy metal stress.....	26
Figure 2.2 Cell division after 24 hours of stress is unaffected.....	27
Figure 2.3 Effect of nutrient stress on the movement of GFP from the phloem.....	28
Figure 2.4 Fluorescent profile of GFP across the root transition zone.....	29
Figure 2.5 Restriction of GFP movement in response to high iron is reversible and correlates with the presence of callose in the phloem.....	30
Figure 2.6 Aniline blue staining of callose after 24 hours of stress treatment.....	32
Figure 2.7 Analysis of GFP diffusion coefficient in response to heavy metal stress.....	33
Figure 2.8 Callose phenotypes and mRNA levels of CalS and β -1,3-glucanase mutants tested.....	35
Figure 2.9 Effect of excess iron on callose deposition and movement in <i>cals5</i> and <i>cals12</i> lines.....	36
Figure 2.10 CFDA transport in <i>cals5</i> and <i>cals12</i> lines.....	37
Figure 2.11 Effect of excess copper on callose deposition and movement in <i>bg_ppap</i> and <i>bg6</i> lines.....	38
Figure 2.12 The β -1,3-glucanases BG_PPAP and BG6 are not required for recovery of roots from excess iron.....	39
Figure 2.13 Growth of the primary root is inhibited by excess copper or iron.....	40
Figure 2.14 <i>cals5</i> mutants are less sensitive to the growth inhibiting effect of excess copper than wildtype.....	41
Figure 2.15 Growth of roots on excess iron inhibits the rate of primary root growth.....	42
Figure 2.16 β -1,3-glucanase mutants are more sensitive to the growth inhibiting effect of excess copper than wildtype	
Figure 2.17 Treatment of roots with excess zinc has no effect on primary root growth.....	45

Figure 2.18 β -1,3-glucanase mutants have normal cellular phenotypes after 24 hours of excess copper47

Figure 2.19 β -1,3-glucanase mutants accumulate excess copper in root tip compared to wildtype.....49

1. INTRODUCTION

There are holes in the sky
Where the rain gets in
But they're ever so small
That's why the rain is thin.

~Spike Milligan

How organisms sense environmental signals and integrate them into developmental outputs continues to be a large question in biology. For plants, which are literally rooted to the ground, responding appropriately to environmental changes is crucial. An early response to environmental challenges is the modification of intercellular signaling; conditions like cold, heat, wounding, and pathogen infection all result in a rapid decrease in cell-cell transport. However, we still do not fully understand the molecular mechanisms, genetic basis, or the biological advantages to this regulation.

As global soils increasingly suffer from heavy metal accumulation due to anthropogenic activities, understanding responses of the plant root system under heavy metal stress is particularly relevant. This project focuses on determining how intercellular signaling via plasmodesmata is regulated in *Arabidopsis thaliana* roots under heavy metal stress, and elucidating the molecular mechanisms and genetic basis for this regulation. Here I will describe the importance of plasmodesmata-mediated signaling in the contexts of development and stress, and what is known about the effects of heavy metal stress on plant roots.

Metal contamination of soils

Soil quality is negatively impacted by scarcity of essential nutrients or heavy metal contamination. While there have always been naturally occurring sources of metal deposition such as the weathering of rock or volcanic activity, current human activities like industrial processing, agricultural use of fertilizers, mining, waste, and coal burning greatly outweigh natural contributions to metal concentrations in soil, making these environmental stressors increasingly relevant (62, 78, 122). Copper-rich manure and copper-based fungicides, along with zinc-rich sewage all contribute to the presence of heavy metals on farmland soils, which has a direct effect on crop plants (2, 6, 24). In China, agricultural soils are contaminated with cadmium, mercury, and lead produced from anthropogenic activities (143). In Tanzania, the Msimbazi River valley, which is used for vegetable farming, contains chromium, lead, cadmium, and copper (90). These conditions exist in the United States as well. A study taking 3,045 soil samples from across the US found high copper levels in the organic soils of Florida, Oregon and the Great Lakes, high nickel concentrations in serpentine soils of California, and high lead and zinc in the lower Mississippi River Valley (57). These problems have led to large, long-term, and expensive projects to clean up soils. In 1980, the United States EPA launched the Superfund program to clean up contaminated sites, costing between \$335 million and \$681 million per year (www.epa.gov/superfund).

Studying how plants respond to heavy metal stress is an important endeavor; not just to better understand the cell biology of plant mechanisms, but because increased industrial practices, climate change, and the continued rise of global population levels make food security a very real challenge. Major federal agencies such as the USDA's National Institute of Food and Agriculture (www.nifa.usda.gov) continue to fund projects that address food availability.

Plant uptake of metals

Studies in plant metal uptake systems have been largely limited to yeast expression studies and mutant analysis. Because of this, we have little direct evidence for metal uptake and transport *in planta*, and molecular components such as metal receptors, sensors, and ligands are still unidentified for many metals. Here I will describe what is known regarding the uptake of copper, iron, and zinc, the main focus of this work.

Copper is taken up by the root via the COPPER TRANSPORTER (COPT) family of transporters. In soils copper exists in its oxidized form Cu (II), but before transport is reduced to Cu (I). Several lines of evidence have led to the prevailing model that reduction is mediated by FERRIC REDUCTASE OXIDASE (FRO), however FRO reduction of Cu (II) has yet to be directly shown (23, 88). The COPT family is differentially regulated in response to specific copper levels; COPT1 is induced upon copper starvation, while COPT1, COPT2, and COPT4 are induced upon copper excess. Because *copt1* has impaired copper uptake, these mutants are insensitive to excess copper concentrations and retain normal root growth under these conditions (115). The transporter HEAVY METAL P-TYPE ATPASE (HMA5) is strongly and specifically induced by copper, and has a role in copper detoxification and compartmentalization. *hma-5* mutants cannot appropriately distribute excess copper, and are hypersensitive to copper excess, but not other metals (4).

Plants deploy two different strategies for the uptake of iron. Strategy I is a reduction strategy, used by dicots and non-grass monocots. It involves using proton pumps to acidify the rhizosphere surrounding the root, increasing the solubility of Fe (III), which is then reduced to Fe (II) by FERRIC REDUCTION OXIDASE (FRO). Fe (II) is then transported through the plasma membrane of the epidermis via IRON-

REGULATED TRANSPORTER1 (IRT1). Strategy II, used by grass monocots, involves chelation. The root secretes phytosiderophores (low molecular weight compounds related to mugineic acid), which chelate Fe (III). The Fe (III)-phytosiderophore complex then enters the roots via specific transporters.

Zinc is also thought to be solubilized through acidification of the rhizosphere and secretion of chelators, but unlike for copper and iron, these mechanisms are less understood. Zinc transporters responsible for acquisition have been identified in yeast (ZRT1 and ZRT2) and humans (ZIP4 and ZIP10) (48, 79, 142), but in *Arabidopsis*, half of the ZINC-REGULATED TRANSPORTER, IRON-REGULATED TRANSPORTER PROTEINS (ZIPs) family is induced under zinc deficient conditions (51). Thus, which members of the ZIPs are involved in zinc uptake remains to be elucidated, but the current model, based mostly on yeast studies (141), is that the ZIP member IRT1 non-selectively takes up zinc (as well as cadmium).

The rhizosphere, the few millimeters of soil immediately surrounding the plant root, also influences metal uptake. As discussed, roots exude compounds like nucleases into the rhizosphere that increase the solubility of minerals (7). Additionally, bacteria in the rhizosphere increase the root surface area and uptake capacity, and stimulate root hair production (40, 148). They may also contribute to acidification of the rhizosphere by producing chelating agents that increase solubility (161). Additionally, some plant species rely on relationships with beneficial mycorrhizae for improved nutrient uptake and defense against excess metal absorption (83, 119).

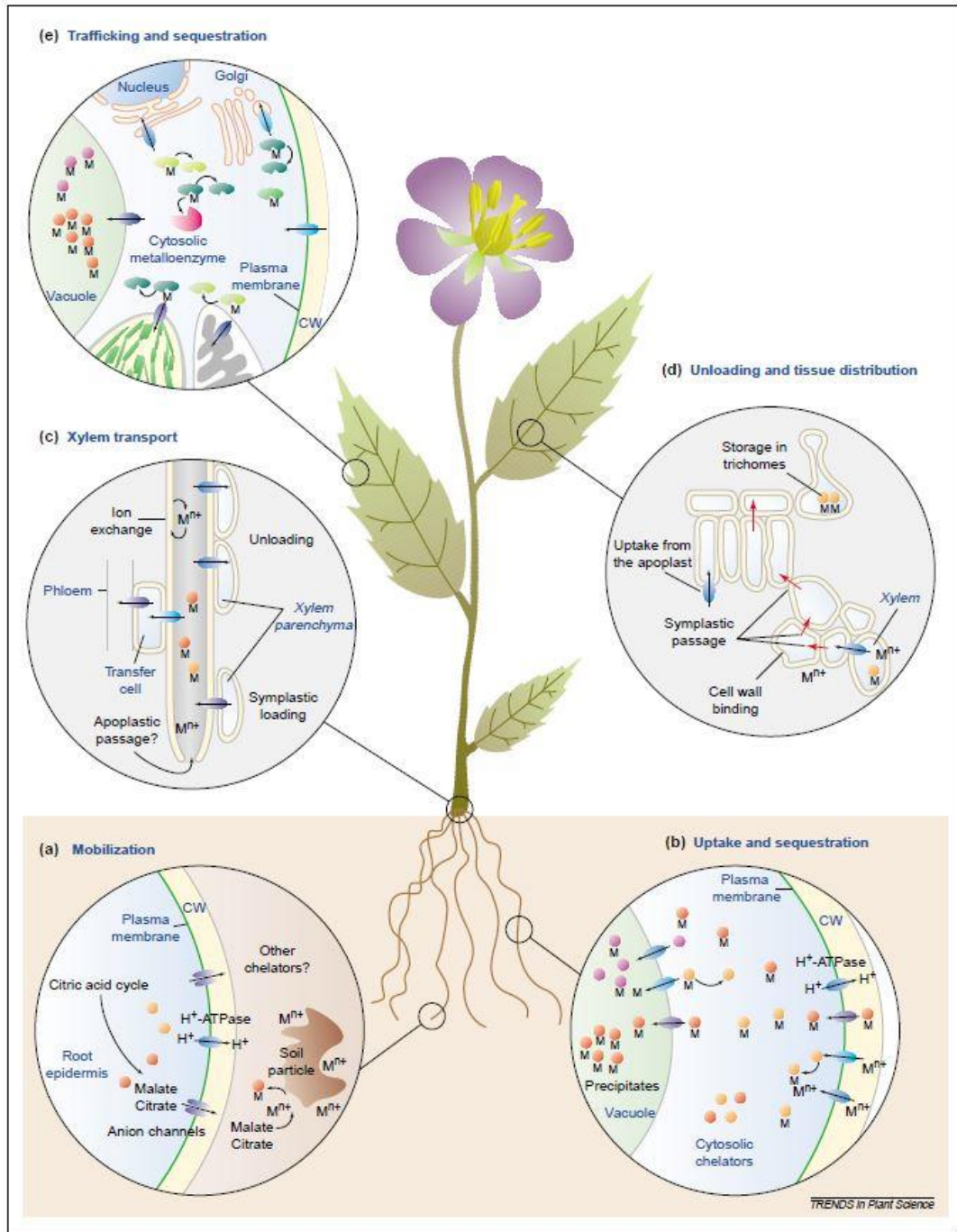


Figure 1.1 taken from Clemes, et al., 2002. Mechanisms of metal accumulation by plants. Metal ions are (a) mobilized by secretion of chelators and acidification of the rhizosphere, then (b) taken up by various uptake systems in the root plasma membrane. (c) Metals are then transported to the shoot via the xylem. (d) Once in the leaf, metals are distributed between cells through plasmodesmata. (e) Reuptake into leaf cells again is catalyzed by various transport systems.

Long-distance transport of metals

All nutrients, including metals, must enter through the root, and subsequently be distributed to appropriate tissues. Long-distance transport of metals involves entering the root, traveling radially until reaching the vasculature, being loaded into the xylem and moving towards the shoot, then being loaded into the phloem to be transported to final destinations, including the root organ (Figure 1.1, taken from Clemens, *et al.*, 2002).

After entering the root, metals are always bound to ligands; less than one free copper or zinc ion exists per cell (126). Metal transport involves the handoff of metal ions from ligand to ligand, making ligands the drivers of intracellular and long-distance transport. Ligands can be proteins, small peptides, or amino acids. Phytochelatins are oligomers synthesized by the enzyme phytochelatin synthase in response to copper or cadmium. Metallothioneins are proteins with a high amount of cysteines arranged in metal-binding motifs, and their expression is induced by copper, cadmium, and zinc. Some metals also use specific chaperones; copper transport uses the metallochaperone CCH (86), while zinc is not predicted to use any metallochaperone proteins. Nicotianamine (NA) chelates copper in the xylem sap, and is involved in copper, iron, and zinc phloem loading and unloading (103). Iron travels in the xylem as a Fe-citrate complex, and through the phloem as Fe-NA (103, 120).

Radial transport of metals in the root has been presumed to rely on both the apoplastic and symplastic pathways (Figure 1.2). Because of suberized and lignified casparian strip, the endodermis is impermeable to metal ions, and they must instead move via the symplasm (155). However, in tissues like the root apex, where the casparian strip is not yet formed, metals may also move through the apoplast (129). Apoplastic movement involves movement from the cell wall plasma membrane into the

cytosol, which is not selective. Thus, while both the apoplast and the symplast contribute to metal levels throughout the plant, the symplastic pathway is thought to control the selectivity and extent of metal movement (22). After reaching the xylem, metals are loaded into xylem cells for distribution to the rest of the plant. While xylem loading of zinc and cadmium is relatively well understood, the identity of transporters for other metals such as copper is still the subject of debate (60, 67, 126, 146).

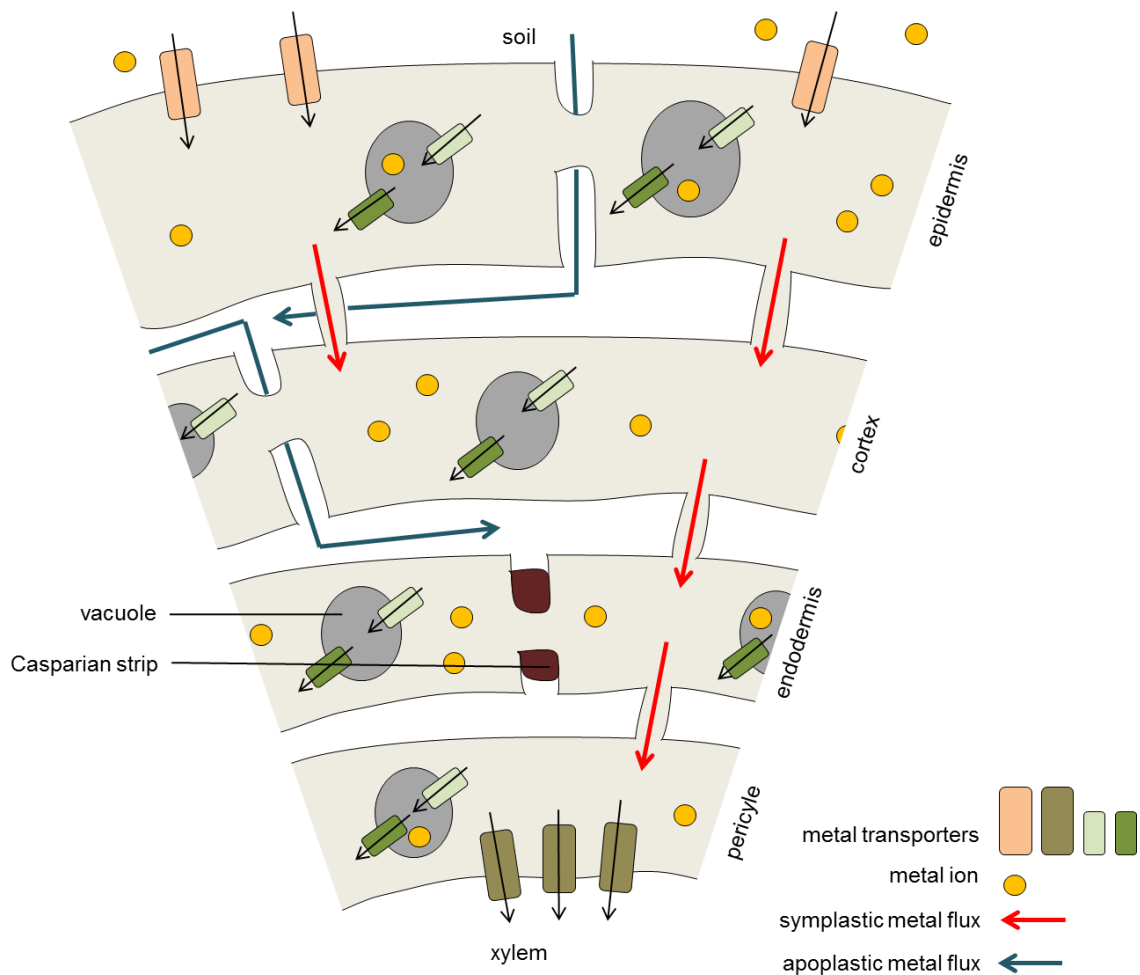


Figure 1.2 General model of radial transport of heavy metals in the root. Symplastic and apoplastic routes of metal transport from the epidermis to the xylem.

Root Responses to Metal Excess

One of the most easily observable plant responses to nutrient stress is the modification of the root system architecture. Many stresses have effects on primary root growth, lateral root length and abundance, and root hair production. Metal excess generally leads to the suberization of root tissue and formation of apoplastic barriers, inhibition of primary root growth, and enhanced lateral branching. Although the inhibition of primary root growth is a general response, the mechanism for how it occurs can vary according to stress. In the cases of lead, mercury, and cadmium stress, there is a decrease in cell division (81, 100, 163). Under copper stress, decreased potassium uptake in the leaf and the accumulation of sugar leads to reduced photosynthesis which in turn reduces root growth (97). Other effects on root system architecture are also stress-specific. Cadmium toxicity decreases the diameter of the root and changes in cell shape (83, 133), lead results in a thickening and blackening of the root, high manganese suppresses root hair formation (70), and in maize, excess nickel leads to an increase in the number of cortical cell layers (84).

Prior to observable anatomical changes in root systems, nutrient status perception and stress signaling must occur. The transcription factor SPL7, which contains a metal-sensing domain and is required for activation and repression of copper-responsive genes, is proposed to sense copper levels (154). How plants sense iron and zinc status is still unknown.

The production of reactive oxygen species (ROS) is a general response and important signaling component under many stresses. Under excess metal stress, ROS are produced through the Haber-Weiss and Fenton reactions, which can be catalyzed by redox metals directly, or as a result of metabolism alterations. Copper and iron, which are redox-active metals, catalyze the conversion of hydrogen peroxide H_2O_2 to $\bullet OH$,

hydroxyl radical, which is highly reactive. Zinc, which is a redox-inactive metal, creates ROS indirectly by inhibiting ROS scavenging mechanisms (12, 29, 96, 102, 140, 162). While prolonged and excess ROS accumulation results in cell death, ROS is also an upstream signal mediator and induces stress-responsive genes (29). Interestingly, the subcellular localization, quantity, and species of ROS determine the specificity of the cellular response (44); this may partially explain why there is such contradictory data in the literature regarding ROS levels and localization under metal stress.

Plants have evolved mechanisms to mediate the detoxification of metals, most of which revolve around keeping excess metal away from important cytosolic components. Movement of metals into the root can be restricted through the action of mycorrhiza, which defend against excess metal absorption (119). To restrict metals from entering the cell, flux across plasma membranes is reduced, coupled with active efflux into the apoplast, where metals can bind to the cell wall (52). Inside the cell, metals are shunted to appropriate subcellular compartments. Metals and metal-ligand complexes are pumped into the vacuole via NRAMP transporters that move cadmium, iron, manganese, and zinc, with low substrate specificity (74, 135, 136).

Metal accumulation in plants

In addition to metal allocation to appropriate subcellular compartments, metals may be sequestered into specific tissues or organs. A few examples show that where metal is distributed under conditions of excess has important implications for plant development.

In maize, excess nickel preferentially accumulates in the pericycle and endodermis of the root. Hyperaccumulation in these root tissues prevents nickel from reaching the aboveground organs. The high accumulation in the pericycle is responsible

for restricted root branching, a response that is unique to nickel toxicity. After 7 days of nickel treatment, plants have 0 lateral roots, even under the mildest concentration of 15 μM nickel, compared to an average of 23 under control conditions (121).

Because Indian mustard (*Brassica juncea*) is a high biomass crop, it is of interest for potential use in phytoremediation (the technique of using plants that can accumulate heavy metals in harvestable shoots, thereby cleaning the soil of metal contamination). In this species, cadmium preferentially accumulates in the trichomes of young leaves, a possible detoxification mechanism, since trichomes are an external tissue. Because ABA treatment reduces cadmium accumulation in the leaf, it is likely that transpiration and mass flow are responsible for cadmium accumulation in the leaf (114). Manganese in sunflower (14) and lead in tobacco (85) also accumulate in trichomes, and in bean, trichomes express a metal-binding metallothionein (43).

Plasmodesmata structure

Signaling between cells is an essential feature of all multicellular organisms to coordinate development and respond to changes in their environment. There was a time where plant cells were thought to be boring, independent units that were trapped in their cell walls and unable to communicate with each other. Mathis Jacob Schleiden wrote in 1838 that “every plant is an aggregate of completely individualized entities, independent and separate, which are the cells themselves”. Not until 1879, when Eduard Tangl observed strands between cells of the strychnine tree and hypothesized that these strands connected cells “to an entity of higher order” did this view begin to change (68).

In plants, most long-distance intracellular signaling occurs via plasmodesmata, channels that provide cytoplasmic continuity between adjacent cells. During cytokinesis, primary plasmodesmata are formed when endoplasmic reticulum becomes trapped

between cells (this ER spanning adjacent cells is called the desmotubule). Secondary plasmodesmata are formed de novo, independent of cell division, to adjust cell-cell connectivity as needed. The protein and phospholipid composition of the plasmodesmata membrane is unique from the cell plasma membrane, with enrichment and exclusive localization of specific proteins and receptors (50, 107).

All cells in the plant are connected by plasmodesmata, with the notable exception of stomatal guard cells and differentiated xylem elements (72, 98). Plasmodesmata allow for the direct transfer of signaling molecules, nutrients, water, RNAs, proteins including mobile transcriptions factors, chaperones, thioredoxins, and cyclin-dependent kinase inhibitors. Molecules that move through plasmodesmata are said to travel via the symplasm (or through the symplastic pathway). Currently there are several models for how molecules might move through the plasmodesmata (Figure 1.3). Molecules can diffuse through the cytoplasmic sleeve, the space between the plasma membrane and the desmotubule (8, 35, 111, 138). Alternatively, molecules can move through the desmotubule lumen or via the membrane (17, 49).

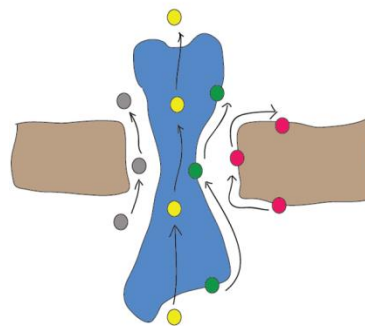


Figure 1.3 Routes of plasmodesmata transport. Models for molecular trafficking between cells include (from left to right) movement through the cytoplasmic sleeve, transport through the desmotubule lumen or membrane, and lateral diffusion along the plasma membrane.

The size of the plasmodesmata aperture determines the extent of cell-cell connectivity by allowing or excluding molecules of certain dimensions. This is referred to as the size exclusion limit (SEL), and while it is mostly based on size, properties such as charge and Stokes radius of the transported molecules play a role as well (5, 42, 134, 145, 156). It has always been thought that stem cell populations and undifferentiated tissues are connected by large SEL, and that as tissues mature and differentiate, the SEL becomes more restrictive (27, 46, 65). However, a recent study has found that new plasmodesmata have a very narrow cytoplasmic sleeve, and that this widening only occurs during cell maturation, suggesting that transport via plasmodesmata is regulated by more than just changes in the SEL (92).

Movement of non-cell-autonomous factors in development

During development, mobile transcription factors traffic between cells to determine cell identity and patterning. Some examples of mobile transcription factors important for normal development are SHORTROOT (SHR), FLOWERING LOCUS T (FT), and CAPRICE (CPC). SHR moves via plasmodesmata from its site of production in the stele to the adjacent cell layers for proper development of the ground tissue (69). When SHR movement from the stele to the endodermis is blocked, roots experience defects in cell division and polarity (151). FT is a transcription factor induced under long days, and important for flowering. It is expressed in the leaves, but its protein acts in the shoot meristem to activate APETELA, a floral meristem identity gene. Early experiments found that when a plant grown under long days was grafted to a non-induced plant, the second plant was able to flower (73, 158). More recent grafting experiments found that FT:GFP expressed in the shoot was found in *ft* roots (25), confirming that the FT protein

is a long-distance signal. CPC moves from its site of production in non-root hair cells to adjacent cells to determine root hair cell fate (71). Because root hairs are the major site of nutrient absorption, the symplastic movement of CPC between epidermal cells is particularly important for both development and the response to nutrient starvation. Indeed, a recent study found that elements of the CPC pathway are responsible for the increase in root hair production observed under low phosphate conditions (116). While these are three classic examples, this is in not a rare phenomenon. Rim, *et al.*, found that 22 out of 76 transcription factors tested were able to move out of their expression domain in the root (109). Small RNA movement through plasmodesmata also has developmental importance. For example, miR165/166 is made in the endodermis, but moves into the stele periphery, degrading its target PHABULOSA (PHB), an HD-ZIP III transcription factor, and creating a gradient of PHB mRNA that determines xylem cell types in a dose-dependent manner (19).

Plasmodesmata transport can occur through passive diffusion or targeted transport. The intercellular transport of some proteins is non-targeted and driven by diffusion, as is the case for LEAFY (LFY), which shows a diffusion gradient with the highest levels in the tissue are where it is produced (152). However, other transcription factors like KNOTTED1 (KN1) (82) and CAPRICE (CPC) (71) can directly increase the plasmodesmata aperture to facilitate their own movement between cells, suggesting a regulated, not passive, movement through plasmodesmata. Other transcription factors require additional factors such as chaperones or interactions with the cytoskeleton or endomembrane for their movement. KN1 requires CCT8, a subunit of a type II chaperonin complex, presumably for refolding after reaching its destination cell (153). Transport of SHR relies on the endomembrane pathway and intact microtubules;

pharmacologically inhibiting early and late endosomes or microtubules disrupts normal SHR movement (149, 150).

Plasmodesmata permeability is carefully regulated during normal developmental processes like flowering, bud dormancy, and organogenesis. In floral development, signals moving symplastically from leaves to shoot apices can promote or repress flowering. Studies analyzing the movement of symplastic tracers show that commitment to flowering correlates with a decrease in tracer movement through plasmodesmata (47). In perennials, the meristem cycles between states of cell-cell communication. Chilling at the end of the growing season, accompanied by shorter days, leads to a closing of plasmodesmata and the development of dormant and freeze-tolerant buds. Breaking dormancy requires the reopening of plasmodesmata, which results in a restoration of the symplastic connections in the meristem. This “dormancy cycling” is important for perennial plants in temperate climates to anticipate regular seasonal changes (110). During lateral root organogenesis, plasmodesmata must be temporarily shut down for the establishment of lateral root primordia. This is likely necessary for forming the auxin gradient required for lateral root initiation in the pericycle. Regulation of cell-cell connectivity in this process determines where lateral roots form, which has implications for root system architecture and nutrient acquisition (10).

Plasmodesmata roles in biotic stress

While plasmodesmata-mediated signaling is regulated by developmental cues, it is also influenced by outside factors. The best studied example of this is in response to pathogenesis. Plants are susceptible to viral, fungal, and bacterial pathogens, and plasmodesmata play an important role in each of these contexts to mediate plant defense and disease symptoms. All viruses encode movement proteins (MP), which are

targeted to plasmodesmata and directly increase the SEL to allow for the spread of their infectious genomes (31). In response, plants shut down plasmodesmata to restrict the spread of infection. Fungi and bacteria (non-viral pathogens), mostly remain in the apoplastic space (with the exception of some fungi having intracellular hyphae that move through plasmodesmata) (123). However, plasmodesmata are crucial for initiating a signaling response. Defense-related pathogen associated molecular pattern (PAMP) receptors are enriched at plasmodesmata, and recognize bacterial proteins like flagellin and chitin to deploy downstream signaling responses. The activation of PAMP receptors triggers a decrease in SEL and decrease in plasmodesmata permeability (39, 87, 107, 144).

Regulating plasmodesmata in response to infection is complex; plasmodesmata closure is necessary to contain pathogen-derived factors, but keeping plasmodesmata open is necessary to propagate response signals. For antiviral RNA silencing to be amplified between cells, small RNAs need to move via plasmodesmata (105). In non-viral pathogenesis, the closing of plasmodesmata is required for immunity. Loss of function of the CHITIN ELICITOR RECEPTOR KINASE 1(CERK1) PAMP receptor, which is required for chitin signaling, leads to an increased susceptibility to infection (45). However, when there is too much plasmodesmata closure, as is observed in the PLASMODESMATA-LOCALIZED PROTEIN (PDLP) PDLP1 or PDLP5 overexpression lines, there is no acquired immunity (18).

Plasmodesmata roles in abiotic stress

Less is known about the importance of modifying plasmodesmata signaling in response to abiotic stress. Most studies have been correlative, showing that exposure to stress results in a decrease of plasmodesmata permeability. While it is easy to

understand why plasmodesmata shut down to prevent pathogen spreading, it is less clear why plants would modify plasmodesmata signaling in response to stresses like pressure, cold, wounding, or nutrient starvation.

Oparka *et al.* (94) showed that plasmodesmata can be sensors of pressure gradients between adjacent cells. By using a micropressure probe/injection system, they created turgor pressure gradients between the trichome cells of *Nicotiana* leaves and assessed the movement of Lucifer Yellow. They found that plasmodesmata transport is strongly blocked when there is a pressure differential between neighboring cells. Conducted in 1992, this was one of the earliest experiments to show that transport via plasmodesmata could be modified in response to exogenous mechanical cues. It was also an exciting study for testing the idea that plasmodesmata can 'sense' local changes in the cellular environment.

Soon after, osmotic stress was shown to induce a transient opening of plasmodesmata. Using pea roots, Schulz, *et al.*, (118) found that after treating root tips with low water potential media there was an increase in the phloem unloading of ^{14}C . Additionally, electron microscopy of mannitol-treated root tips revealed an increase in plasmodesmata diameter under osmotic stress. However, this plasmodesmata widening is short-term; plasmodesmata still returned to their normal diameter whether or not there was continued exposure (3 hours) to osmotic stress. This study was important for showing that plasmodesmata responses can be transient, and not the result of permanently altered cell-cell connectivity. This study is also significant because it is the only recorded condition that causes an increase (instead of decrease) in plasmodesmata transport, albeit a transient one.

Using maize suspension-culture cells, Holdaway-Clarke *et al.* (56) showed that cold treatment causes a spike in cytosolic Ca^{2+} , causing plasmodesmata to go from

open, to shut, to open again in 10 seconds. Ca^{2+} is a second messenger to chilling, and while others had previously used high experimental levels of Ca^{2+} , this was the first report of a rapid change in intercellular signaling in response to cold with physiological levels of Ca^{2+} . Importantly, these results demonstrate how rapid and dynamic gating of plasmodesmata can be; it was a surprising finding that this response could occur in a matter of seconds.

Cui *et al.* (28) showed that mechanical wounding causes a restriction of plasmodesmata transport. After wounding the tips of *Arabidopsis* leaves, there is a 30% decrease in the movement of the symplastic tracer Carboxy fluorescein (CF) after 30 minutes. Interestingly, CF movement begins to recover in as little as 3 hours, with full recovery after 24 hours. These experiments indicate that blocks to plasmodesmata can be transient and reversible, enhancing our understanding of the dynamic regulation of intercellular signaling in response to external cues. This study was also important to the field for identifying specific genes that mediate the changes in plasmodesmata connectivity (discussed further below).

Müller *et al.* (89) published the first report showing that a nutrient signal, in the form of phosphate starvation, effectively blocks the movement of a mobile transcription factor. Using *Arabidopsis* seedlings they found that SHR:GFP movement into the quiescent center (QC) is restricted under low phosphate conditions in as soon as 12 hours. Separate from this, plasmodesmata also play a role in deploying the low phosphate response. miR399, the master regulator of the phosphate starvation signaling module, allows for the expression of high-affinity phosphate transporters to increase nutrient uptake. Grafting experiments and examination of phloem sap strongly suggest that the miR399 moves from the shoot to root to execute this response (80, 99). Because of this long-distance transport, miR399 is presumed to move via

plasmodesmata from the shoot to root to increase phosphate uptake. Thus plasmodesmata signaling plays a role in phosphate starvation in both allowing movement of miR399 from shoot to root, and blocking movement in and out of the QC.

These studies show that plasmodesmata responses to abiotic cues can be rapid, occurring in a matter of seconds or minutes, and reversible. Over the years, our paradigm of plasmodesmata as static structures has evolved into an understanding of these channels as rapid and dynamic responders to a variety of signals. Additionally, the literature suggests that under stress, plasmodesmata permeability is generally decreased (with osmotic stress being an exception). It is still unclear what, if any, is the biological benefit to the changes in plasmodesmata signaling observed under many of these conditions.

Regulation of plasmodesmata signaling

To date, the best understood and most studied regulator of plasmodesmata permeability is the polysaccharide callose. Callose is a β -1,3-glucan, and when induced is deposited to plasmodesmata, effectively decreasing the plasmodesmata aperture and restricting macromolecular traffic between cells (Figure 1.4, taken from Tilsner, *et al.*, 2016). The presence of callose at plasmodesmata is a reflection of the activities of two enzyme families. Callose synthases (CaS) use UDP-glucose as a substrate to synthesize callose, while β -1,3-glucanases degrade callose by catalyzing callose hydrolysis. Callose is involved in normal developmental processes such as pollen development, cell plate formation and functional megaspore selection (33, 36, 63, 93).

The CaS enzymes contain multiple transmembrane domains and a cytosolic loop with a putative UDP-glucose binding site. CaSs interact with *trans*-partners that

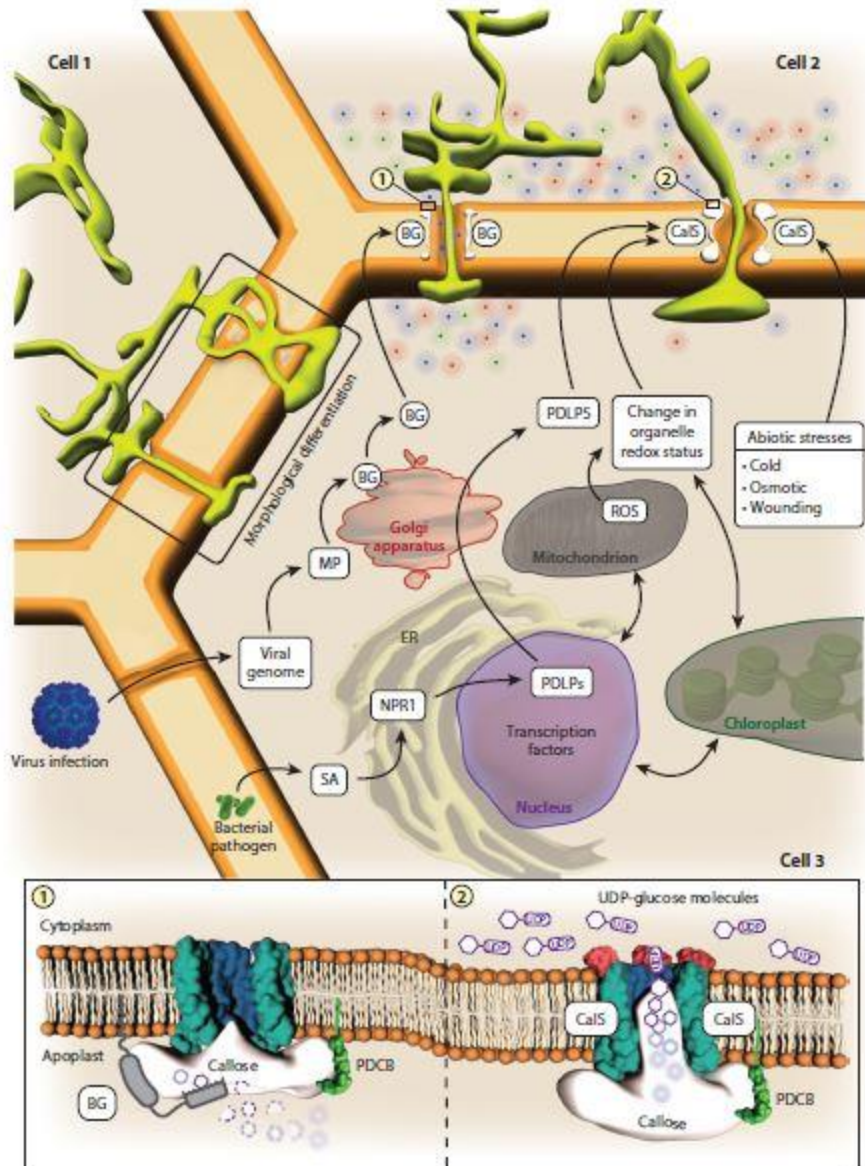


Figure 1.4 Mechanisms of plasmodesmata regulation, taken from Tilsner, et al., 2016. Regulatory mechanisms that lead to 1) open and 2) closed plasmodesmata states. Redox states of the cytosol and organelles, cytosolic calcium, phytohormones, and pathogen infection are signaling nodes that regulate callose-mediated changes in size exclusion limit. Additionally, morphological differences in plasmodesmata structure (simple or branched) shown in left, affect macromolecular transport via plasmodesmata.

together form the CalS holoenzyme complex. While most *trans*-factors are still unknown, to date a UDP-glucose transferase (58), a sucrose synthase (1), and annexins (3) have been identified. The differential regulation of specific CalSs, together with interaction of specific *trans*-partners has been suggested as a way to exert specific regulation of callose synthesis.

Arabidopsis has 12 CalS genes, and the field is starting to piece together their specific roles in responding to environmental signals. CalS8 responds to wounding stress using hydrogen peroxide (H₂O₂) as a signal (28), CalS1 is activated by the salicylic acid pathway to respond to pathogen infection in the leaf (28), and CalS12 deposits callose plugs at sites of fungal penetration (61). The unique roles elucidated thus far for individual CalS genes indicate possible subfunctionalization of the CalS members.

The β -1,3-glucanase enzymes in *Arabidopsis* are a much larger family, consisting of 50 predicted members. Structurally, these enzymes contain an N-terminal glycosyl hydrolase family 17 domain (GH-17) which catalyzes callose hydrolysis. The C-terminal contains a callose binding domain (X8) or a carbohydrate-binding module 43 (CBM43). Less is known about the specific roles for individual β -1,3-glucanases, in part because they are such a large family. However, BG_PPAP has been linked to viral spreading in the leaf. In *bg_ppap* mutants, callose deposition was increased after viral infection, and viral spreading was reduced (76). In roots, PLASMODESMATA LOCALIZED β -1,3-GLUCANASE (PdBG1 and PdBG2) are responsible for callose turnover that reestablishes symplastic connectivity during lateral root organogenesis (10).

In addition to CalS and β -1,3-glucanase enzymes, GPI-anchored plasmodesmata callose-binding proteins (PDCB) influence callose accumulation at plasmodesmata.

While they have no enzymatic activity, PDCB proteins bind callose through their CMB43 domain, stabilizing callose at the plasmodesmata neck region (125). PDBGs and PDCBs are both membrane-bound via GPI anchors, reinforcing the model that specific protein composition at the plasmodesmata membrane influences molecular trafficking through plasmodesmata (50). A partial *Arabidopsis* cell wall proteome analysis identified PDLPs a family of plasmodesmata localized proteins with features of type I membrane receptor-like proteins. Later, PDLP5 was found to mediate plasmodesmata closure in response to pathogen infection in a salicylic acid-dependent manner (28, 75)

While callose is an important player in developmental and environmental responses, very little is known about how the enzymes responsible for callose accumulation are themselves regulated. Correlative studies have linked calcium and ROS signaling to activation of the CalS enzymes (11, 128). Accumulation of ROS stimulates a cytosolic influx of Ca^{2+} , and increases in cytosolic Ca^{2+} can lead to plasmodesmata closure, as is the case after exposure to cold (56). However, we still do not know how these signals are integrated at the plasmodesmata and then transmitted to the CalS enzymes. Cold and wounding result in the accumulation of callose in seconds or minutes, suggesting that regulation occurs at the level of protein activity (28, 56). In the case of β -1,3-glucanases, less is known. However, according to Doxey, *et al.* a small group of β -1,3-glucanase genes are regulated at the level of transcription in response to hormone treatment, ozone stress, bacterial or pathogen infection (34).

Other molecules, subcellular domains, and structural differences can regulate cell-cell connectivity, although many of these aspects are still not well understood. First, the change in plasmodesmata from a simple to a complex structure, as occurs in leaves undergoing a sink-source transition, can influence symplastic transport between cells. In tobacco leaves, branched plasmodesmata restrict non-specific plasmodesmata transport

(95). Conversely, the INCREASED SIZE EXCLUSION LIMIT 1 (ISE1) mutants, which have increased transport of fluorescent tracers, also have a higher frequency of twinned plasmodesmata (131).

Secondly, like plasma membranes, cell walls can have microdomains with specific compositions that lead to different mechanical properties. For example, plasmodesmata pit fields, which are sites of high plasmodesmata transport and cell-cell exchange, have cell walls with low cellulose and high pectin content, which facilitate the function of forming secondary plasmodesmata (26, 38).

Thirdly, the cytoskeleton components actin and myosin have been found to localize to plasmodesmata, and dye diffusion experiments show that disrupting either of these leads to alterations in the normal SEL (132). However, it is still unknown if the actin cytoskeleton controls plasmodesmata aperture directly, or if this effect is indirect through protein recruitment, microdomain organization, or membrane shaping.

Lastly, plasmodesmata membrane contact sites (MCS) have been more recently studied and proposed to greatly influence symplastic permeability. MCS are areas where two membranes are in very close proximity (30nm) but do not fuse, and in plant cells, the MCS between the ER desmotubule and plasmodesmata membrane is particularly relevant (54, 104). MCS tethers are protein complexes that connect the two membranes and mediate this interaction. These MCS tethers adjust the gap between membranes, determining the space available for macromolecular transport (55). Shortening of the gap between the ER and PM can facilitate crosstalk if the membranes are close enough, and models have been suggested for receptor-induced Ca^{2+} signaling at ER/PM MCS (20). Importantly, MCS have been shown to respond to environmental cues; the synaptotagmin SYTA is recruited to the ER/PM MCS during viral infection, and is necessary for the accumulation of MP at plasmodesmata during viral infection (77).

In summary, plasmodesmata-mediated transport is essential for plant life, and tightly regulated in both development and in response to abiotic and biotic stress. Since Tangl's prescient findings in 1879, the paradigm of plant intercellular communication has completely changed, and we have come to appreciate plasmodesmata function and importance. However, there is still much we do not fully understand about how plasmodesmata are regulated, and the molecular components and signaling pathways that lead to this regulation. While the effects of pathogenesis on plasmodesmata transport have been well studied, less is known about the effects of nutrient stresses. Further work is needed to elucidate if there is a biological or adaptive benefit to plasmodesmata modification in other contexts. Additionally, it is still unclear if shutting down plasmodesmata is a universal response to stress, since only a few conditions have been studied. The identification of genes that regulate plasmodesmata permeability is being actively pursued by the field, and there are several lines of evidence that suggest subfunctionalization of the enzymes that regulate callose turnover at plasmodesmata in response to specific environmental cues.

While heavy metal contamination is an increasingly relevant environmental stress, we still do not know how it affects plasmodesmata transport. Even components such as metal receptors, sensors, and ligands are still unidentified for many metals, and we do not have a full understanding of how metals are taken up by the root and move within the plant. However, one relevant mechanism is the finding that metals such as aluminum, nickel, and cadmium preferentially accumulate in different tissues or organs. Since metals presumably use the symplastic pathway for their long-distance movement and distribution, it is likely that plasmodesmata play a role in the proper distribution of metals.

2. RESULTS

Plasmodesmata-mediated transport is modified under conditions of nutrient stress.

To determine whether a decrease in plasmodesmatal permeability is a general response to nutrient stress we transferred 5-day old *A. thaliana* seedlings to media lacking essential nutrients: 0 μM phosphate, 0 μM iron or 0 μM zinc or media containing excess nutrients: 600 μM iron, 150 μM zinc, or 50 μM or copper. In addition, we examined the effects of 85 μM cadmium, which competes against other metals for uptake into the root but plays no role itself in normal plant nutrition. After 24h on the stress media, we assessed the effects of these treatments on the movement of carboxyfluorescein diacetate (CFDA) or free GFP through plasmodesmata.

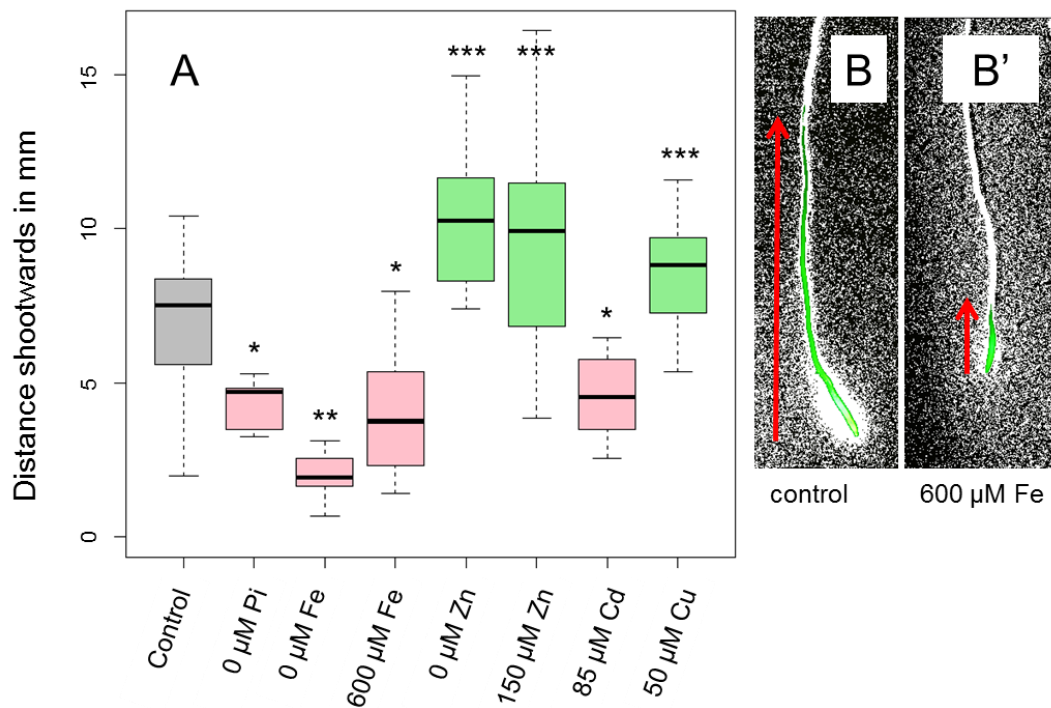


Figure 2.1 Changes in CFDA transport after heavy metal stress. (A) Distance of CFDA transport shootwards after 24 hours of stress treatment. Wilcoxon rank sum test, $p < 0.05$, $n = 25$ or greater. (B)-(B') Sample image of CFDA after color threshold has been applied using ImageJ under (B) control or (B') 600 μM Fe.

CFDA is a commonly used small (~ 1kD) symplastic tracer. When applied to the root tip, CFDA is internalized and converted to the fluorescent molecule, carboxy fluorescein (CF). CF traffics between cells exclusively via plasmodesmata. Under our assay conditions, when CFDA was micropipetted (2.0 μ L) directly onto the tip of an unstressed root, CF moved rapidly into the epidermis and cortex cell layer and then shootward up the root an average of 68.0 mm (Figure 1 A and B). In roots that have been grown for 24 h on 0 μ M phosphate, 0 μ M iron, 600 μ M iron, or with 85 μ M cadmium movement of CF was significantly reduced, suggesting that these growth conditions elicited a decrease in plasmodesmata permeability (Figure 2.1, A and B'). In contrast, roots grown on 0 μ M zinc, 150 μ M zinc or 50 μ M copper all increased the distance that CF traveled from the root tip, indicating an increase in plasmodesmata permeability (Figure 2.1, A).

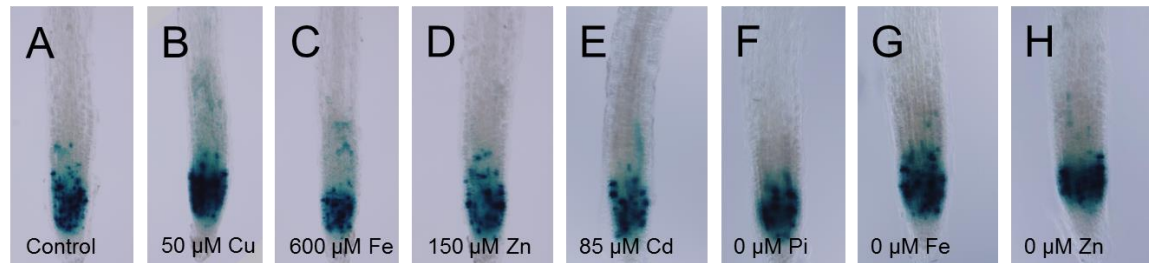


Figure 2.2 Cell division after 24 hours of stress is unaffected. GUS staining of *cycb1;1:GUS* line, marking actively dividing cells, after 24 hours of (A) control conditions, (B), 50 μ M Cu, (C) 600 μ M Fe, (D) 150 μ M Zn, (E) 85 μ M Cd, (F) 0 μ M Pi, (G) 0 μ M Fe, and (H) 0 μ M Zn.

None of these growth conditions (paucity or excess) affected the levels of cell divisions in the root meristem (Figure 2.2). Likewise, with the exception of the 0 μ M phosphate treatment, which dramatically increased the frequency of emerged root hairs, none of these treatments affected the overall patterning of the root. These results suggest that the changes that we see in the movement of CF in response to nutrient

stress are not the result of general changes in the development of the root meristem, but rather modifications in plasmodesmatal permeability.

Free (untagged) GFP (~27 kD) is able to move between most cells in the plant via PD (117). As such, movement of GFP is used as a marker of symplastic signaling. Under normal growth conditions, when GFP is expressed in the phloem companion cells using the SUCROSE-H⁺ SYMPORTER 2 (SUC2) it is unloaded into the pericycle and diffuses via plasmodesmata throughout the entire root meristem (Figure 2.3A and Figure 2.4).

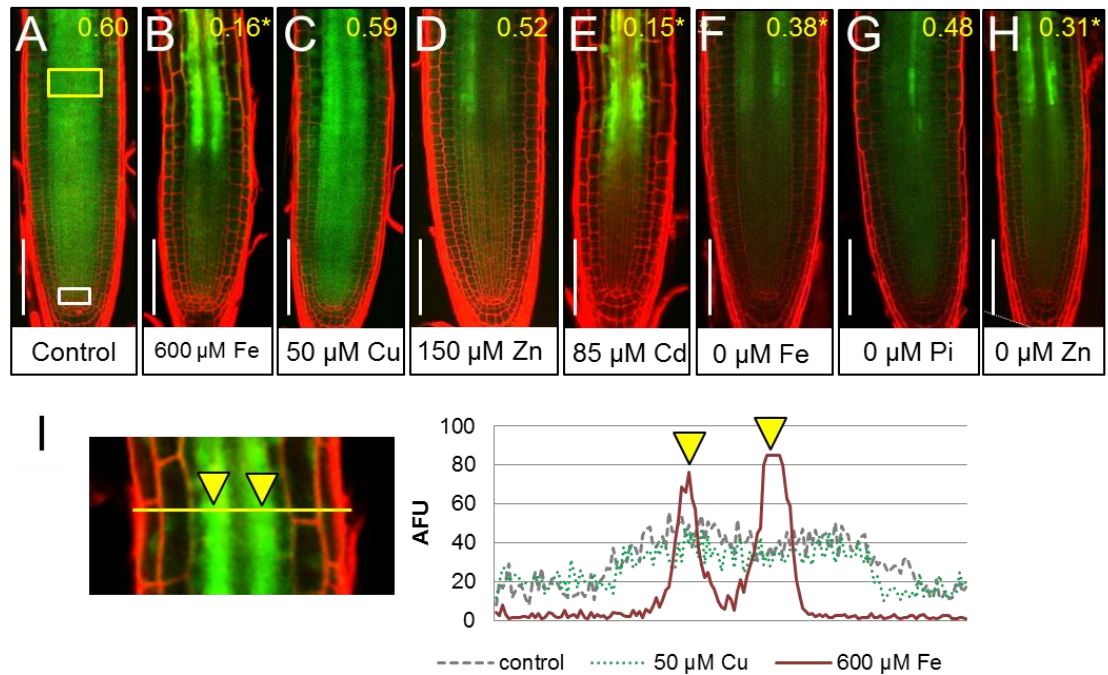


Figure 2.3 Effect of nutrient stress on the movement of GFP from the phloem. (A-H) SUC2:GFP expressing 6 day old seedlings at 24 h after transfer to (A) standard MS (control) (B) 600 μM iron (C) 50 μM copper (D) 150 μM zinc (E) 85 μM cadmium (F) 0 μM iron (G) 0 μM phosphate, and (H) 0 μM zinc. Scale bar 75 μm. Inset values are the ratio of mean GFP mean fluorescence intensity in the stele of the root tip just above the QC (white boxed region) relative to the stele in the transition zone of the root (yellow boxed region); *indicates statistical significance, 2-tailed t-test, p<0.05. (I) Arbitrary fluorescence units (AFU) of GFP radially across the transition of the root in representative samples: control, 50 μM copper, and 600 μM iron.

In roots with defective trafficking however, GFP fluorescence is largely limited to the phloem (9, 89). In our assays, growth of roots for 24 h on 50 μ M copper, 150 μ M zinc or 0 μ M phosphate had no appreciable effect on movement of GFP out of the phloem or its distribution in the root meristem (Figure 2.3C, D, G, and I; Figure 2.4B). In contrast 24 h treatment of roots with 0 μ M iron, 0 μ M zinc, 600 μ M iron, or 85 μ M cadmium all reduced the movement of GFP from the phloem (Figure 2.3B, E, F, H and I; Figure 2.4A).

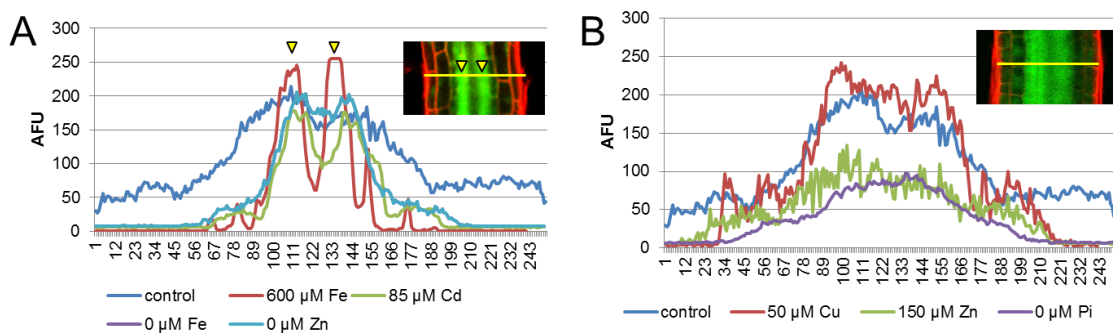


Figure 2.4 Fluorescent profile of GFP across the root transition zone. Arbitrary fluorescence units (AFU) of GFP in a line across the transition zone of a 6 day old root 24 h after growth on media (A) that decreases the QC to stele ratio of GFP fluorescence: 600 μ M iron, 85 μ M cadmium, 0 μ M iron or 0 μ M zinc (as labeled) or (B) under conditions that have no effect on movement of GFP 50 μ M copper, 150 μ M zinc and 0 μ M Pi. Control roots are shown in both graphs.

This is reflected in the decrease in the movement of GFP into the meristem (the ratio of GFP fluorescence in the stele above the QC relative to the stele where the phloem extends into the meristem; QC:P ratio) and a change in the fluorescence intensity profile of GFP radially across the transition zone of the root meristem compared to the controls (Figure 2.3 and Figure 2.4). In roots with a decreased QC:P ratio (in control roots the QC:P ratio is 0.60) there is conspicuous peaks in GFP signal in the two phloem strands (indicated by yellow arrow-heads in Figure 2.3I and Figure 2.4). These

results indicate that short term exposure of roots to 0 μM iron, 0 μM zinc, 600 μM iron or 85 μM cadmium decreases plasmodesmatal permeability in the post-phloem domain of the root meristem. The block to movement of free GFP in these assays is not the result of permanent changes to plasmodesmata; the restriction of GFP movement is reversible. For example, when roots grown for 24 h on 600 μM iron are allowed to recover on control media for 24 hours, GFP profiles return to the normal pre-stressed levels (Supplemental Figure 2.5, A-C).

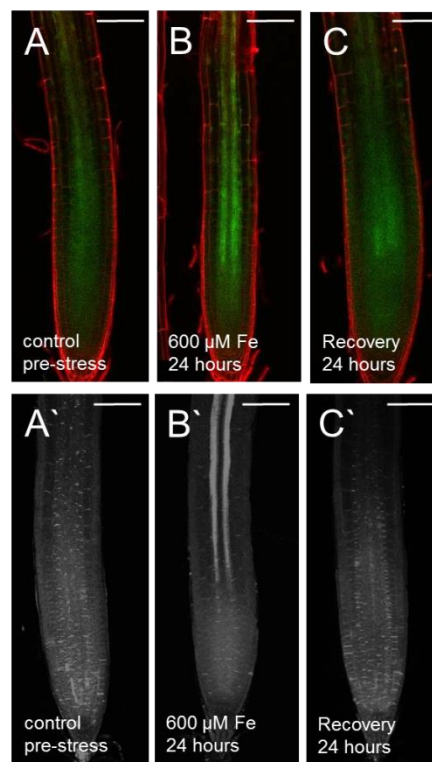


Figure 2.5 Restriction of GFP movement in response to high iron is reversible and correlates with the presence of callose in the phloem. (A -C) SUC2:GFP seedlings stained with (A' -C') aniline blue. (A and A') prior to iron treatment, (B and B') after 24 hours on 600 μM iron, and (C and C') after 24 h recovery on normal media for 24 hours. (Scale bar 100 μm).

Collectively these data indicate that while many stressors trigger a decrease in plasmodesmata permeability, a restriction in plasmodesmata-mediated trafficking is not in fact a universal response to abiotic stress.

Changes in the accumulation of callose drive the response of the root to iron and copper.

The β -1,3-glucan, callose, has emerged as a major regulator of plasmodesmata permeability. When deposited at plasmodesmata, there is a general decrease in the size of plasmodesmatal apertures, and restricted movement of macromolecules between cells. To determine if any of our growth conditions affect the accumulation of callose in the root, we stained roots with aniline blue, a fluorescent dye that binds callose (157).

In the root meristem, callose is apparent in the walls of newly divided cells; however low basal levels of callose are found surrounding all cells under normal growth conditions (Figure 2.6A). Short-term (24 h) growth of roots on 85 μ M cadmium, 0 μ M iron, 0 μ M zinc, and 150 μ M zinc had no quantitative effects on callose levels in the root meristem, elongation or differentiation zones (Figure 2.6D-F, H and I). There were also no obvious qualitative differences in the deposition of callose. In contrast, growth of roots on 50 μ M copper induced a general decrease in the levels of callose in the root meristem, elongation and differentiation zones (Figure 2.6C and I), which correlates with the observed increase in movement of CF that is seen in Figure 1. Growth of roots on 0 μ M phosphate resulted in a tissue-specific accumulation of callose, in the epidermis of the differentiation zone of the root, particularly among the root hairs (Figure 2.6G). Previous reports by Müller showed a marked increase in aniline blue staining in the QC region of 6 day-old roots grown for 48 h on 0 μ M phosphate; we did not observe this as a general phenomenon - one root of 17 showed conspicuous accumulation of callose

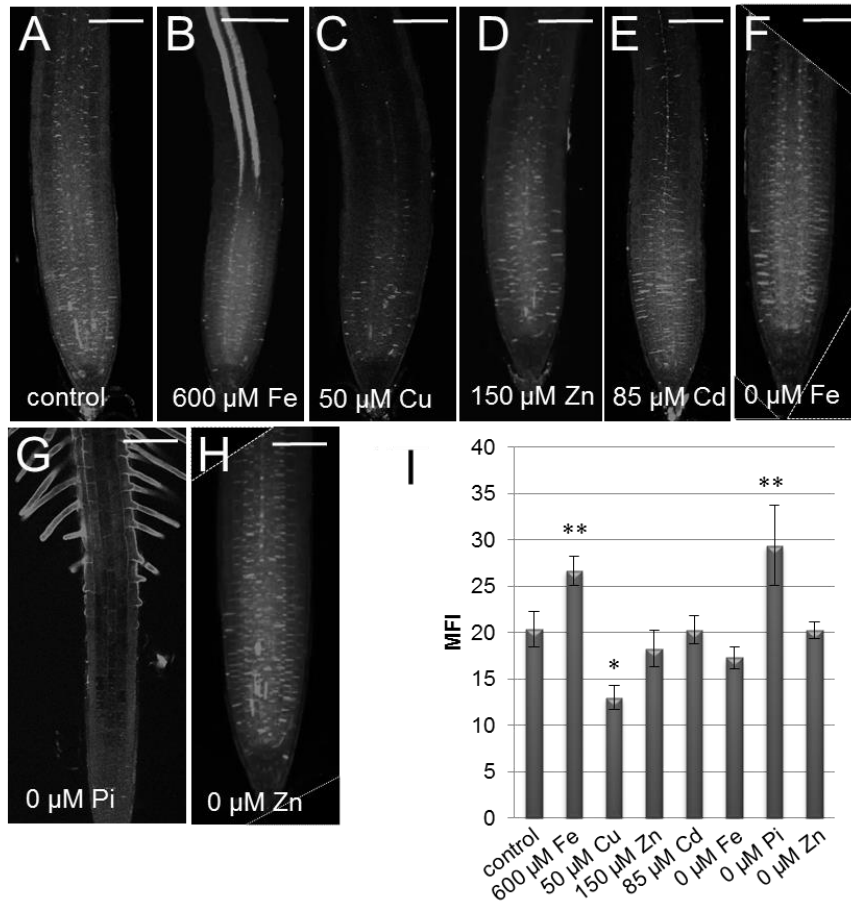


Figure 2.6 Aniline blue staining of callose after 24 hours of stress treatment.

Aniline blue staining of callose after 24 h transfer to (A) standard (control) MS media (B) 600 μM iron (C) 50 μM copper (D) 150 μM zinc (E) 85 μM cadmium (F) 0 μM iron (G) 0 μM phosphate, and (H) 0 μM zinc. Scale bar 100 μm . (I) Mean fluorescence intensity (MFI) of aniline blue signal in roots treated as indicated. 2-tailed t-test, $p < 0.05$, $n > 19$, error bars indicate standard error.

around the QC. Growth of roots for 24 h on 600 μM iron resulted in a dramatic and tissue-specific increase in callose in the phloem, with no obvious qualitative changes in aniline blue staining in other regions of the root (Figure 2.6B). Interestingly the deposition of callose in response to high iron was reversible. When roots were removed from media containing 600 μM iron and allowed to recover for 24 h on normal MS medium, callose levels return to normal (Figure 2.5A`-C`). The iron induced buildup and

turnover of callose correlates with the observed inhibition and recovery of GFP movement (Figure 2.5A-C).

To further assess the relationship between heavy metal stress and protein movement, we examined movement of free GFP (using Raster Imaging Correlation Spectroscopy) within a defined region of the root meristem of roots treated for 24 h with 600 μM iron, 50 μM copper, or 150 μM zinc.

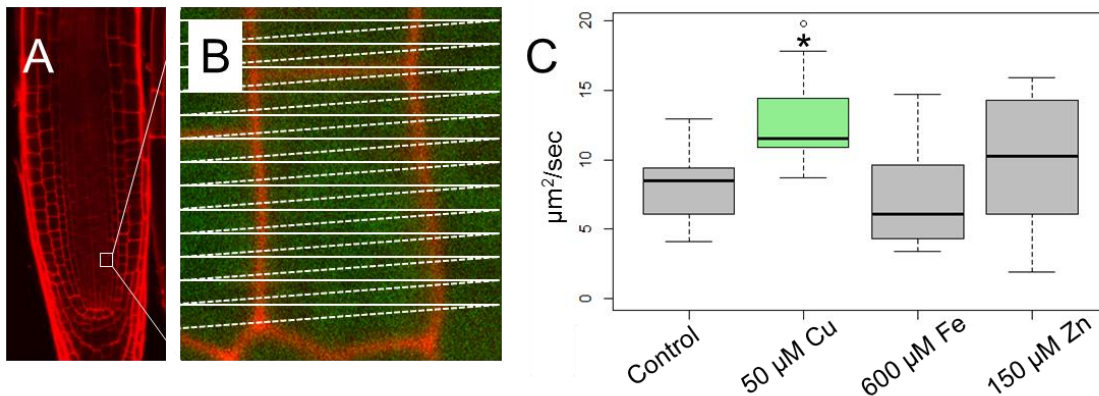


Figure 2.7 Analysis of GFP diffusion coefficient in response to heavy metal stress. (A) Small white box shows region of interest (ROI) used for RICS. (B) Magnified representative image of an ROI in which RICS was performed. (C) Average diffusion coefficients for GFP in 35S:GFP seedlings after 24 h of treatment with 50 μM copper, 600 μM iron or 150 μM zinc. 2-tailed t-test, $p < 0.05$, $n > 14$.

In the region of interest used for RICS we saw no effects on callose levels in response to iron or zinc treatment and a decrease in callose in the copper treated roots. In control roots the diffusion coefficient of free GFP in the region of the meristem tested (shown in Figure 2.7A) was 7.94 $\mu\text{m}^2/\text{sec}$, which is consistent with previously published results (21). Within the same region of interest in the 600 μM iron or 150 μM zinc treated roots, there were no quantitative difference in the levels of callose compared to the controls and no difference in the coefficient of diffusion in these roots compared to the controls (Figure 2.7C). In contrast, there was a general decrease in callose levels in the

region of interest of roots grown on 50 μM copper and a significant increase in the coefficient of diffusion of free GFP (Figure 2.7C). These results suggest that growth of roots on 600 μM iron causes a tissue specific increase in callose and a block to movement of GFP out of the phloem (Figure 2.3), but not a general decrease in plasmodesmatal permeability in the stele (Figure 2.7), whereas growth of roots on excess copper have generally decreased callose levels in the root meristem and increased plasmodesmatal permeability.

Callose synthases and β -1,3-glucanases control the levels of callose in response to excess iron and copper.

Callose accumulation is regulated by two families of enzymes; callose synthases, which synthesize callose, and β -1,3-glucanases, which degrade callose. Recent data suggest that at least for the callose synthase family, specific genes are responsible for responding to specific cues. To identify genes involved in the response of *A. thaliana* roots to excess iron or copper we tested the ability of callose synthase and β -1,3-glucanase mutants to respond to 24 h treatment with 600 μM iron or 50 μM copper respectively (Supplemental Figure 4).

There are 12 annotated callose synthase (*CalS*) genes in *A. thaliana*. We were able to isolate viable homozygous loss-of-function lines for 10 of the 12 family members. *cals9* nulls are gametophytic lethal (59); loss of *cals10* is seedling lethal (113). As in previous assays, *cals* seedlings were grown for 5 days on standard MS media and then transferred for 24 h to media containing 600 μM iron. After 24 h on 600 μM iron, roots were stained with aniline blue and assessed for the induction of phloem-specific callose and a general increase in the levels of callose in the root meristem. Here 8 of the 10 *cals* lines showed a wildtype response to growth on excess iron (Figure 2.8).

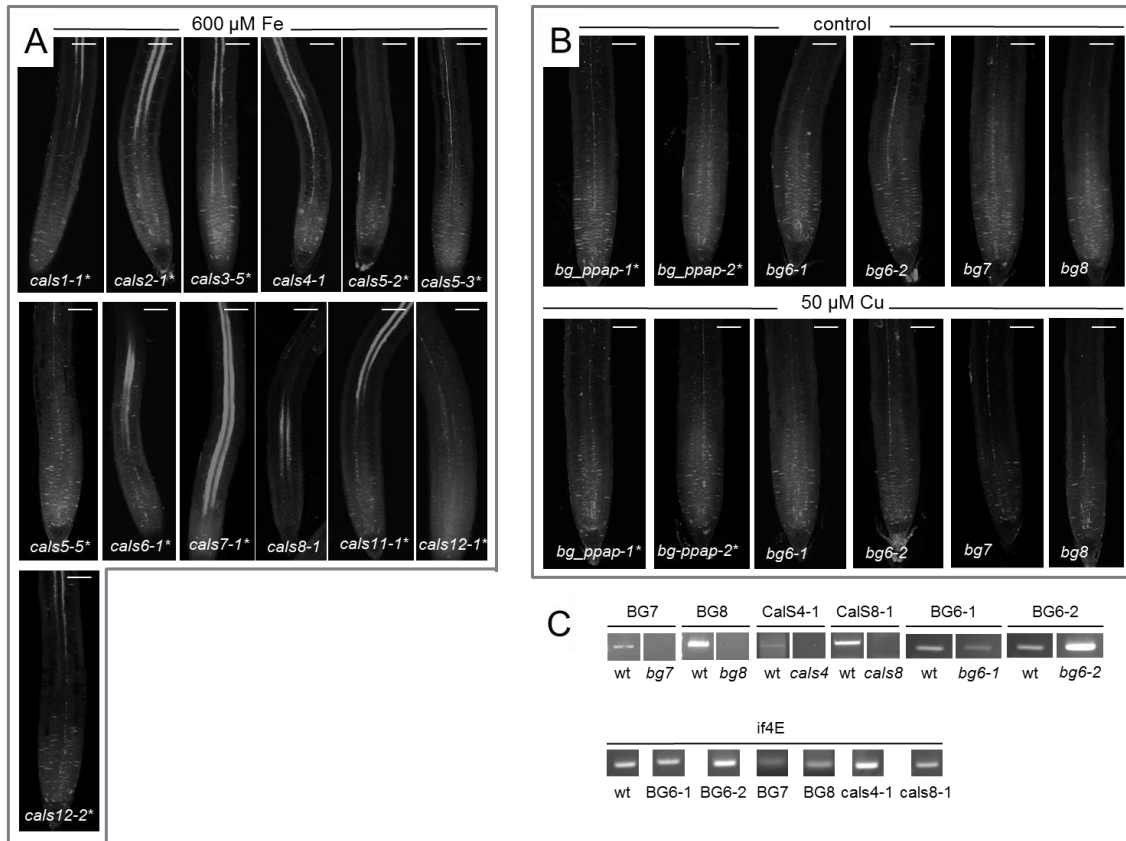


Figure 2.8 Callose phenotypes and mRNA levels of CalS and β -1,3-glucanase mutants tested in this study. Aniline blue staining of roots, genotypes as indicated 24 h after treatment with (A) 600 μ M iron, or (B) 50 μ M copper. Scale bar 75 μ m. (C) Levels of mRNA expression in indicated genotypes after 30 cycles of PCR. *in (A) and (B) indicate published alleles, for which there are no mRNA levels tested in (C).

In contrast, *cals5* (*cals5-2*, *cals5-3* or *cals5-5*) and *cals12* (*cals12-1* or *cals12-2*) showed an attenuated response to excess iron (Figure 2.9). Despite a decrease in the basal levels of callose in the *cals5* lines, the *cals5* roots were still responsive to treatment with excess iron showing a 31% increase in aniline blue signal in *cals5-2* lines versus 33% increase in wildtype after 24 h on 600 μ M iron (Figure 2.9D). In addition approximately 50% of the *cals5-2* roots examined showed modest increases in phloem callose compared to wildtype. However, the increases in phloem callose was not

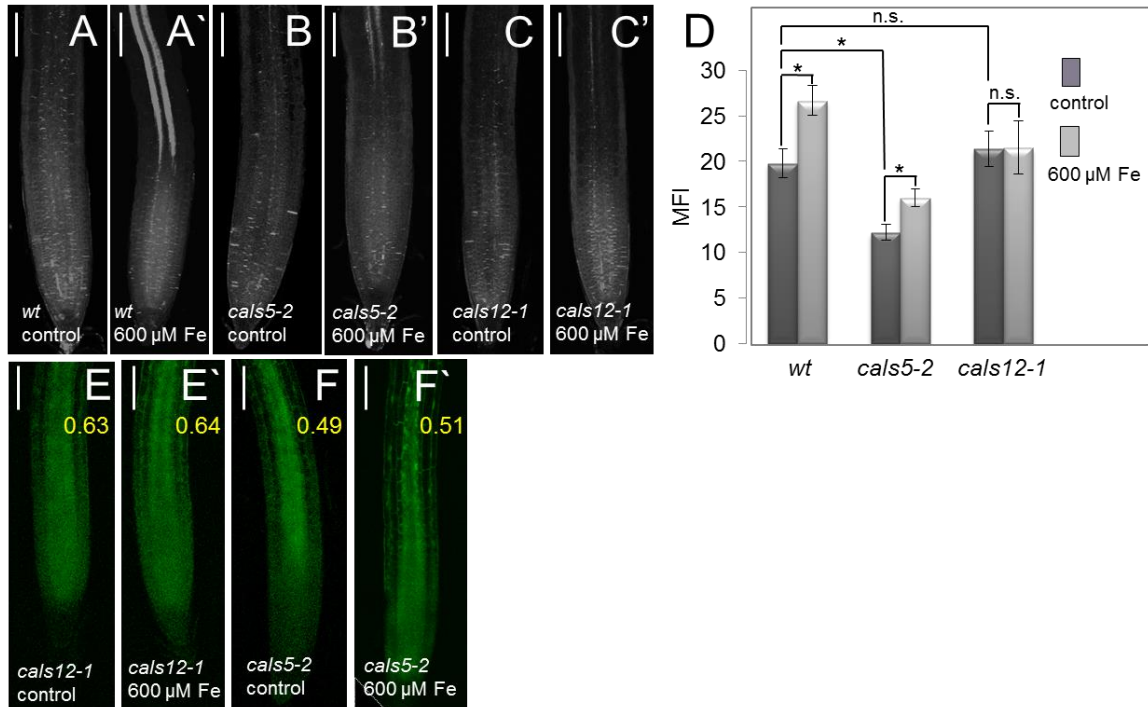


Figure 2.9 Effect of excess iron on callose deposition and movement in *calS5* and *calS12* lines. (A-D) Aniline blue staining of callose in (A and A') wildtype, (B and B') *calS5-2*, and (C and C') *calS12-1* under (A-C) control conditions, and (A'-C') 24 h after treatment with 600 μM Fe. (D) Callose levels after 24 hours of growth in control or 600 μM iron in *calS5-2* and *calS12-1*. 2-tailed t-test, $p < 0.05$, $n = 20$ or greater, error bars indicate standard error. (E-F') SUC2:GFP expressing 6 day old *calS5* and *calS12* seedlings at 24 h after transfer to (E and F) standard MS (control), and (E' and F') 600 μM iron. Inset values are the ratio of mean GFP mean fluorescence intensity in the stele of the root tip just above the QC relative to the stele in the transition zone of the root. Scale bars in A-F' 100 μm.

sufficient to block movement of GFP from the phloem or affect the QC:P ratio (Figure 2.9 F and F'). In contrast, 24 h treatment with 600 μM iron significantly inhibited movement of CF in the *calS5-2* lines. The *calS12* (*calS12-1* or *calS12-2*) roots showed normal basal levels of callose and no quantitative increases in callose levels in response to 24 h treatment with 600 μM iron (Figure 2.9D). Only occasionally (approximately 1 in 10 roots) was there a low level accumulation of callose in the phloem. Consistent with these results, GFP movement from the phloem (SUC2:GFP) is not inhibited by treatment of the

cals12-1 mutants with 600 μM iron (Figure 2.9 E and E'). The *cals12-1* lines however are responsive to iron treatment, as movement of CF is inhibited in the *cals12-1* roots (similar to wildtype) after 24 h on 600 μM iron (Figure 2.10). These results indicate that CALS12 is largely responsible for the iron induced production of phloem specific callose and the subsequent block to the movement of GFP out of the phloem. CALS5 is required for basal callose production in the root, not specifically in the phloem or specifically in response to iron. Additionally, pathways independent of callose may restrict movement of CF within the iron-stressed roots.

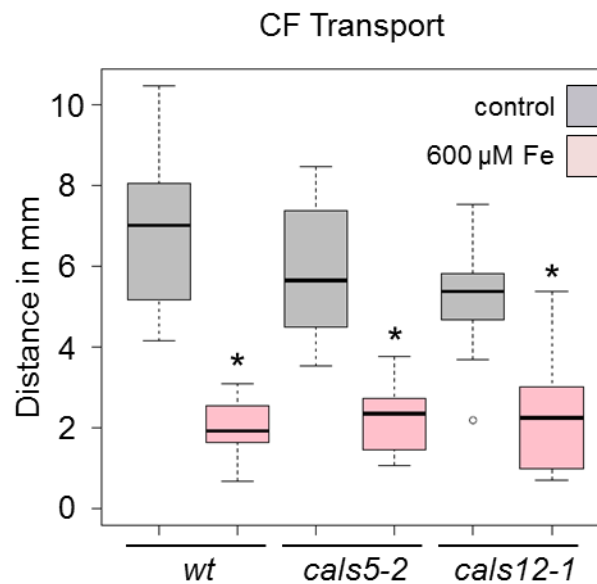


Figure 2.10 CFDA transport in *cals5* and *cals12* lines. Distance of CFDA transport shootwards after 24 hours of treatment with 600 μM Fe (Wilcoxon rank sum test, $p < 0.05$, $n = 25$ or greater).

There are 50 predicted β -1,3-glucanases in *A. thaliana* (34). Doxey et al., 2007, divided the β -1,3-glucanases into 13 groups (A-M). Here we concentrate our analysis on the group D β -1,3-glucanase genes, which are specifically expressed in the root, and regulated in response to various stress conditions. In addition, we examined BG_PPAP, a stress-responsive plasmodesmata-localized β -1,3-glucanase that is not part of the

group D β -1,3-glucanases (76). As in previous assays, the loss-of-function lines were grown for 5 days on regular MS media before being transferred for 24 h onto media containing 50 μ M copper. Neither *bg_ppap-1* nor *bg6-1* (At4g16260) showed a reduction in callose levels or an increase in CF movement that is seen in wildtype roots in response to 50 μ M copper treatment (Figure 2.11) indicating that both *BG_PPAP* and *BG6* are required for wildtype responses to excess copper.

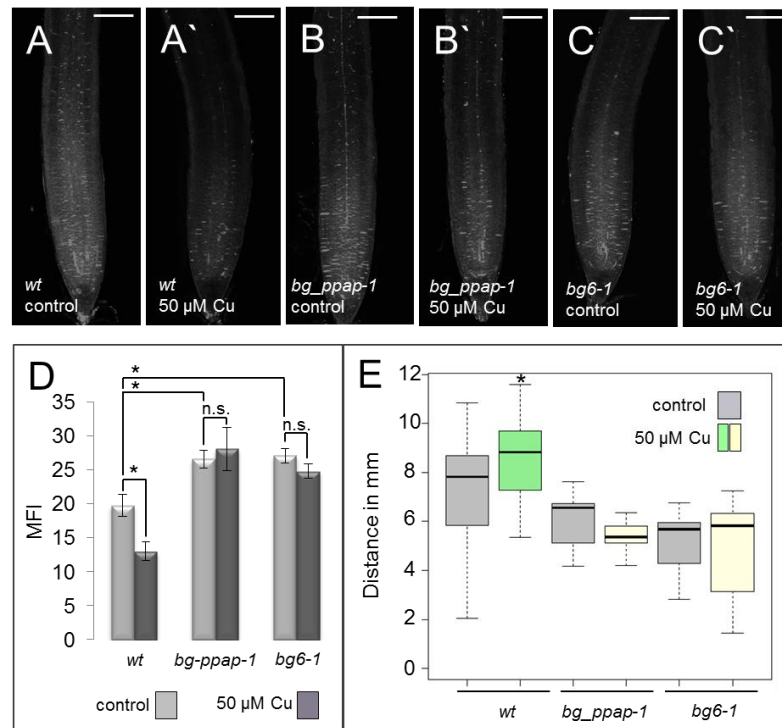


Figure 2.11 Effect of excess copper on callose deposition and movement in *bg_ppap* and *bg6* lines. Aniline blue staining of callose (A-C) under normal growth conditions, and (A'-C') after 24 h treatment with 50 μ M Cu. Scale bar 100 μ m. (D) Callose levels after 24 hours of control or 50 μ M Cu in *bg_ppap-1* and *bg6-1*. 2-tailed t-test, $p < 0.05$, $n = 20$ or greater, error bars indicate standard error. (E) CFDA transport shootwards in *bg_ppap-1* and *bg6-1* (Wilcoxon rank sum test, $p < 0.05$, $n = 25$ or greater).

However, *BG_PPAP* and *BG6* are not generally required for response to heavy metal stress or the breakdown of callose. Both *bg_ppap-1* and *bg6-1* show normal

increases in phloem specific callose after 24 h of growth on 600 μM iron (Figure 2.12A` and B`). More importantly after 24 h recovery on normal MS media (Figure 2.12A`` and B``) callose is broken down normally in the phloem of the *bg_ppap* and *bg6-1* lines. These results suggest that *BG_PPAP* and *BG6* mediate a reduction in callose levels in response to excess copper; however neither is required for breakdown callose during recovery from iron. These data are consistent with callose synthases and β -1,3-glucanases specifically regulating callose levels in response to heavy metal stress, and they further support the premise that changes in callose underlay changes in plasmodesmatal permeability.

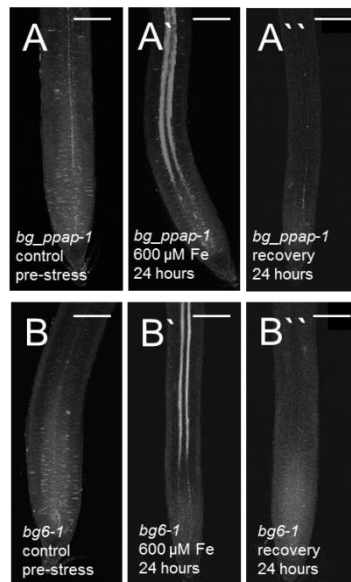


Figure 2.12 The β -1,3-glucanase *BG_PPAP* and *BG6* are not required for recovery of roots from excess iron. Aniline blue staining of (A-A``) *bg_ppap-1* and (B-B``) *bg6-1* (A and B) prior to stress exposure, (A` and B`) after 24 hours of 600 μM Fe, and (A`` and B``) after 24 hours of recovery on control media. Scale bar 100 μm .

Modifying plasmodesmatal permeability in response to iron or copper stress has consequences for plant growth.

Inhibition of primary root growth is a common response of plants to nutrient stress. There are likely many factors that contribute to the reduction in root growth; however the results of Sivaguru *et al.*, (127) suggest that changes in symplastic signaling may underlie a significant part of the response. This study showed that exposure of wheat to 20 μM aluminum significantly inhibits growth of the primary root. Remarkably this stunting is ameliorated when roots are pretreated with 2-deoxy-d-Glc, an inhibitor of callose and cellulose synthases prior to exposure to 20 μM aluminum (127). These findings are consistent with speculation in the literature that the production of excess callose in response to abiotic stress is generally inhibitory to growth.

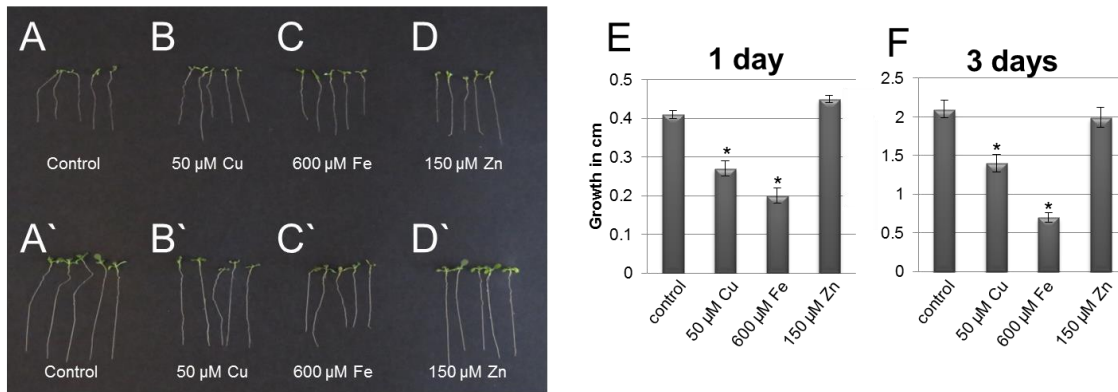


Figure 2.13 Growth of primary root is inhibited by excess copper or iron. Seedlings treated for (A-D) 1 day or (A'-D') 3 days with excess copper, iron, or zinc as labeled. (E-F) Increase in the length of the primary root during (E) 1 day of treatment as labeled, or (F) 3 days. 2-tailed t-test, $p < 0.05$, $n > 14$, error bars indicate standard error.

To examine the connection between nutrient stress, callose, and root growth, we looked at changes in the growth of *A. thaliana* roots after treatments with 50 μM copper, 600 μM iron or 150 μM zinc. As shown in Figure 2.13, both 50 μM copper and 600 μM

iron decrease the rate of root growth (by 35% and 50% respectively at day 1, and by 33% and 70% respectively at day 3); however even after 3 days of growth on 50 μ M copper or 600 μ M iron the root meristems are actively dividing. These results indicate that while short-term growth of roots on excess iron or copper stunts the growth of the primary root, the roots are still alive and actively dividing.

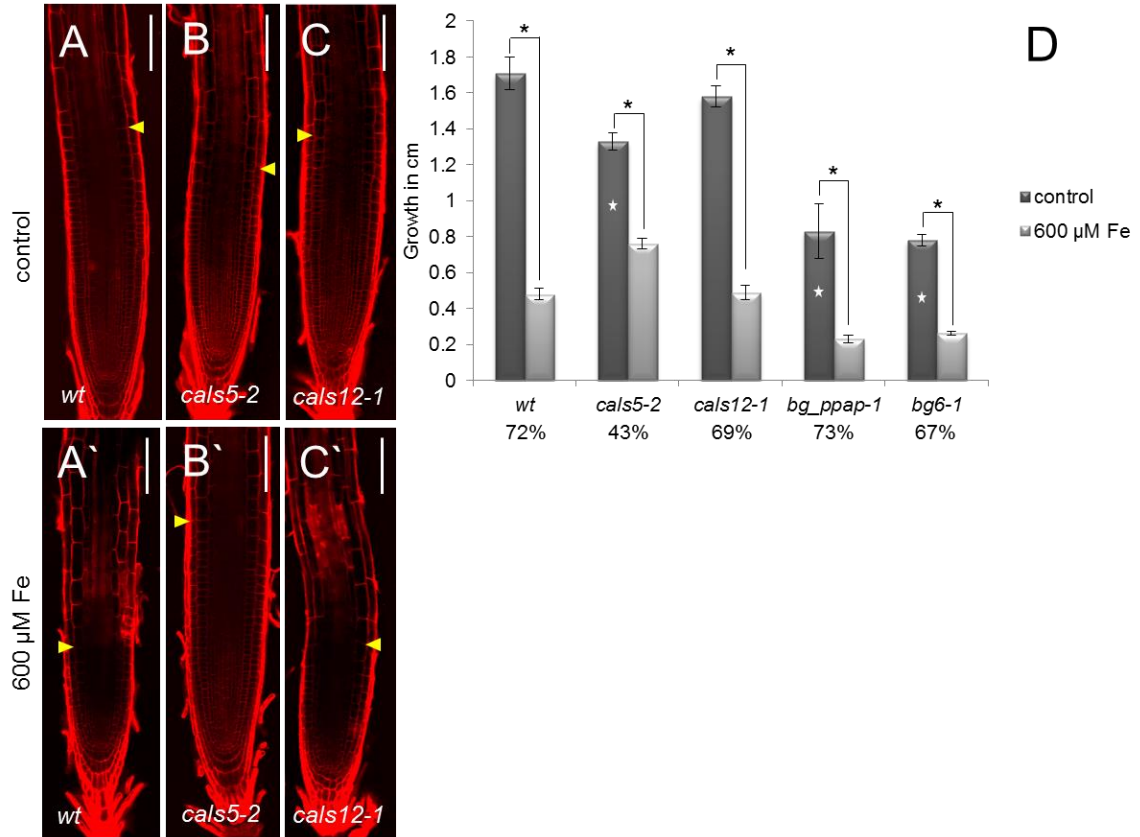


Figure 2.14 cal5 are less sensitive to the growth inhibiting effect of excess copper than wildtype. (A-C) Roots transferred for 3 days to (A-C) regular MS media or (A'-C') media containing 600 μ M iron. Scale bar 100 μ m. The yellow arrow heads indicate the end of the meristematic zone and the beginning of the elongation zone. (D) Increase in the length of the primary root during the 3 days post-transfer to control or media containing of 600 μ M iron. Percentages below the root genotypes indicate percent inhibition of growth relative to MS grown roots. 2-tailed t-test, $p < 0.05$, $n = 15$ or greater, error bars indicate standard error. Star indicates growth statistically less than wildtype under control conditions.

A plausible model for the effect of iron on the growth of the primary root is that increased levels of callose in the phloem decrease the ability of the vasculature to transport molecules needed for growth into the root meristem. To test this model, we examined the effect of 600 μM iron on the growth of *cals5-2* and *cals12-1* roots. As shown in Figure 2.14, the *cals5-2*, but not the *cals12-1* mutants were less sensitive to iron induced inhibition of root growth. This was seen both in the overall reduction in root growth – approximately 72% in wildtype compared to 43% in the *cals5-2* lines (Figure 2.14D) and in the overall size and structure of the root meristem (Figure 2.14B’).

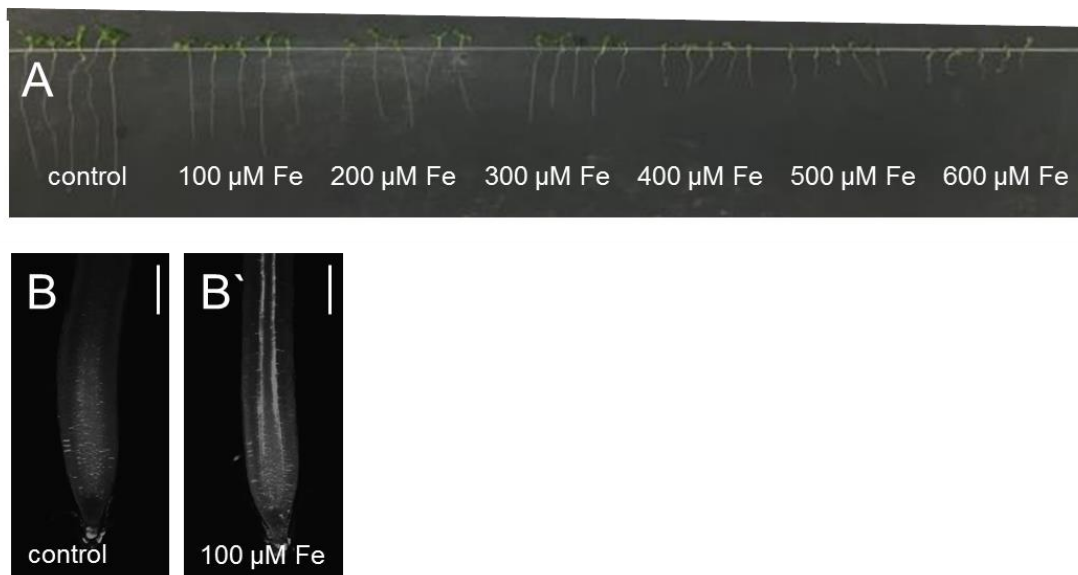


Figure 2.15 Growth of roots on excess iron inhibits the rate of primary root growth. (A) 7 day old wt seedlings germinated directly on standard MS media (control) or media containing excess iron as labeled. (B-B') Aniline blue staining of callose after 24 hours of (B) control or (B') 100 μM Fe. Scale bar 100 μm .

Since the *cals5-2*, but not the *cals12-1* lines still produce callose in response to treatment with 600 μM , with about half of the *cals5-2* roots showing increases in phloem specific callose in response to excess iron, these results are not consistent with our

initial model. Therefore, to further explore the connection between iron-induced callose deposition and inhibition of root growth, we directly germinated and grew wildtype roots for 7 days on media containing between 100-600 μM (in 100 μM increments) iron (Figure 2.15A). In these assays the extent of inhibition of root growth directly correlated with the concentration of iron. However, it did not correlate with the presence of excess callose in the phloem as even roots grown for 24 h on media containing 100 μM showed iron induced accumulation of phloem specific callose (Figure 2.15B'). Collectively these results suggest that the ameliorative effects of the *cals5-2* mutation on inhibition of root growth in response to excess iron are the result of the overall general decrease in callose levels in these lines and not due to a lack of phloem-specific callose deposition. It is possible that the rescue of root growth would be more pronounced in *cals5;cals12* double mutants, however we were not able to isolate viable double mutants. Note that similar to the experiments by Sivaguru *et al.*, we tried pretreating roots with 2-deoxy-d-Glc prior to growth on 600 μM iron; however, in our hands, 2-deoxy-d-Glc had no measurable effect on callose levels in response to 600 μM iron.

Roots grown on 50 μM copper show quantitative decreases in the overall levels of callose in the root and increases in the movement of CF and GFP in the root meristem. Roots grown for 1 or 3 days on 50 μM copper are roughly 30% shorter than corresponding control roots grown on normal MS media, indicating that excess copper is inhibitory to root growth (Figure 2.13). To determine if the observed decreases in root growth are the result of altered callose levels we examined the effects of 50 μM copper treatment on the growth of *bg_ppap-1* and *bg6-1* roots, which have slightly increased basal levels of callose but show no changes in the levels of callose or the movement of CF in response to excess copper. Surprisingly both the *bg_ppap* and *bg6-1* lines are

more sensitive to 50 μM copper than wildtype (Figure 2.16). Both *bg_ppap-1* and *bg6-1* show an increase in the inhibition of primary root growth in response to excess copper relative to wildtype (Figure 2.16D) with dramatic decreases

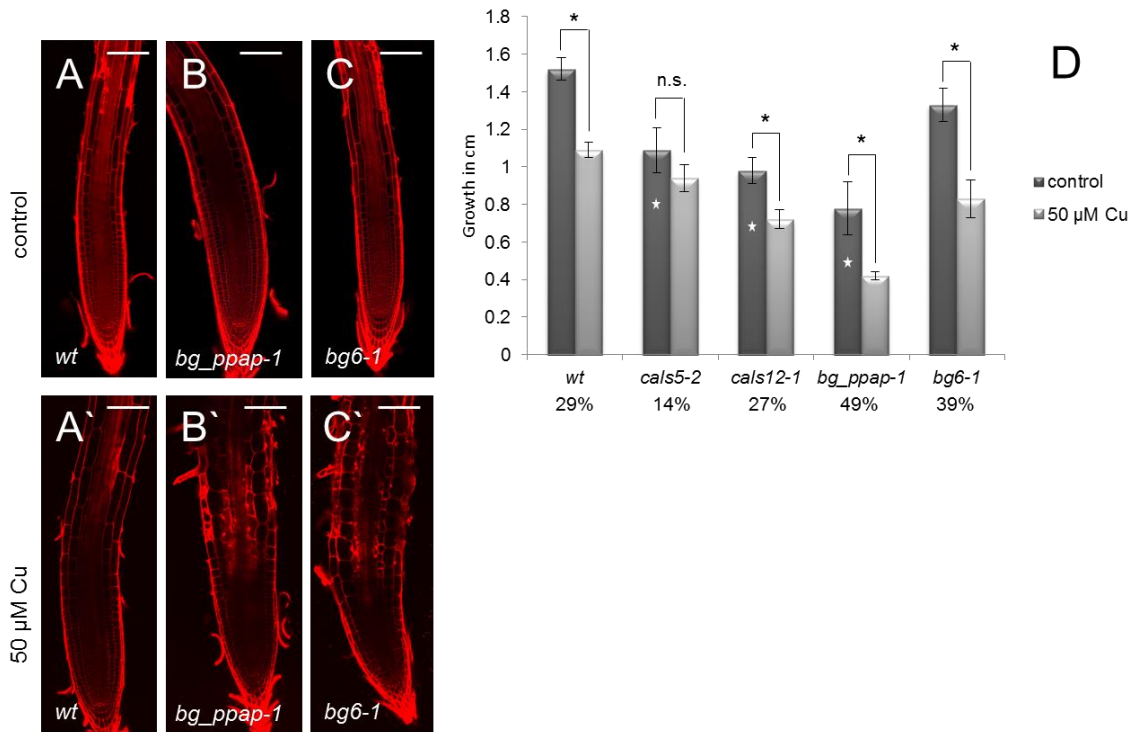


Figure 2.16 β -1,3-glucanase mutants are more sensitive to the growth inhibiting effect of excess copper than wildtype. (A-C) roots transferred for 3 days to (A-C) regular MS media or (A'-C') media containing 50 μM copper. Scale bar 100 μm . (D) Increase in the length of the primary root during the 3 days post-transfer to control or media containing of 50 μM copper. Percentages below the root genotypes indicate percent inhibition of growth relative to MS grown roots. 2-tailed t-test, $p < 0.05$, $n = 15$ or greater, error bars indicate standard error. Star indicates growth statistically less than wildtype under control conditions.

in the size of the meristem, radial swelling in the root elongation zone and cell death (Figure 2.16 A'-C'). Treatment of roots with 150 μM zinc, which also increases plasmodesmatal permeability, but has no effect on callose levels, has no effect on the growth of the primary root (Figure 2.17). These results suggest that rather than inhibiting

growth, the break-down of callose by BG_PPAP and BG6 helps to maintain normal root growth in the presence of excess copper.

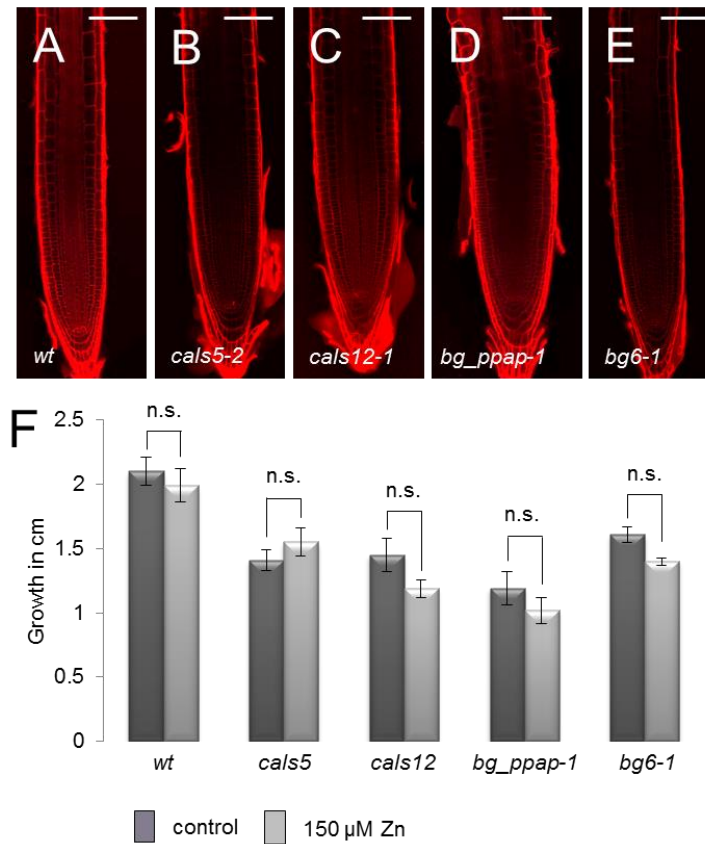


Figure 2.17 Treatment of roots with excess zinc has no effect on primary root growth. (A) wildtype and the (B and C) callose synthase and (D and E) β -1,3-glucanase alleles (as labeled) after 3 days on media containing 150 μ M Zn. Scale bar 100 μ m. (F) Increase in the length of the primary root during the 3 days post-transfer to control or media containing 150 μ M Zn. 2-tailed t-test, $p < 0.05$, $n > 14$, error bars indicate standard error.

If decreases in callose allow for continued growth of the primary root in response to excess copper, then *cal5-2* roots, which have reduced basal levels of callose, should have decreased sensitivity to treatment with 50 μ M copper. Indeed, when 5 day-old *cal5-2* seedlings were grown for an additional 3 days on media containing 50 μ M copper, growth of the primary root was inhibited by only 14%. In contrast, wildtype and

cals12 roots which have normal basal levels of callose show 29% and 27% decreases in the growth of the primary root, respectively (Figure 2.16D). These results suggest that decreases in callose may generally ameliorate stress induced decreases in growth of the primary root. However, the converse was not strictly true. Both *bg_ppap-1* and *bg6-1*, which have increased basal levels of callose, were not more sensitive to the inhibitory effects of 600 μ M iron treatment. Both *bg_ppap-1* and *bg6-1* showed reductions in root growth (73% and 67% respectively) in response to excess iron that were in range with what was seen in wildtype (Figure 2.14). Collectively, these results suggest that increases in callose in response to heavy metal stress generally limit the growth of the primary root and that factors that decrease the accumulation of callose may buffer the inhibitory effects of excess heavy metals on root growth.

The distribution of copper is altered in the β -1,3-glucanase mutants.

Since there are both apoplastic and symplastic routes for the transport of heavy metals, changes in symplastic permeability may alter the distribution of metals within the root. To determine where in the root iron and copper accumulate and determine whether changes in symplastic signaling affect this distribution, we used LA-ICP-MS (Laser Ablation – Inductively Coupled Plasma – Mass Spectrometry), which was recently optimized for use in *A. thaliana* roots (124). For our assays, 10 μ M punches (positioned along a linear grid) were taken from a live *A. thaliana* root; these punches were coupled to MS to determine elemental concentrations in the punches. Assays were done on wildtype and mutant roots under control conditions and after 24 h on excess iron or copper where defects in root growth are minimal and meristem organization is unaffected (Figure 2.18).

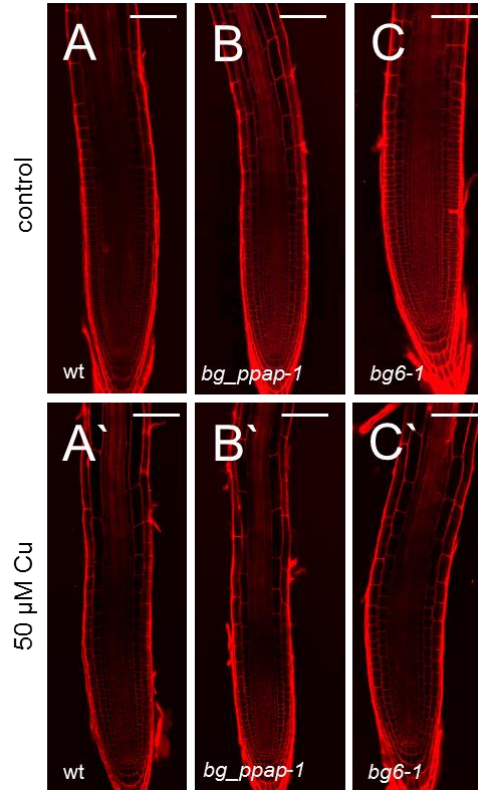


Figure 2.18 β -1,3-glucanase mutants have normal cellular phenotypes after 24 hours of excess copper. (A and A') wildtype, (B and B') *bg_ppap-1*, and (C-C') *bg6-1* treated for 24 hours with (A)-(C) control media or (A')-(C') 50 μ M Cu media. Scale bar 100 μ m.

The roots of wildtype, *cals5-1* and *cals12-1* seedlings were analyzed on control media and after exposure for 24 h to 600 μ M iron. The signals for iron were very low in all genotypes, in all regions of the root. Measurements were similarly low when roots were grown under control conditions or on excess iron. Since others have reported similar challenges with the detection of iron using LA-ICP-MS, this likely reflects a technical limitation of the system and not the biology of the root.

Under normal growth conditions wildtype, *bg_ppap-1* and *bg6-1* all showed similar levels of accumulation of copper throughout the root. After 24 h on 50 μ M copper,

wildtype roots showed increases in copper levels throughout the length of the root with even higher levels in punches 1 and 2, which correspond to the meristem. In root punches 3-10, *bg_ppap-1* and *bg6-1* roots did not differ from wildtype in the levels of copper. In punch 2, levels of copper in *bg_ppap-1* and *bg6-1* were moderately higher than wildtype. However, in the meristem (punch 1) copper levels were dramatically (2-2.5 fold) higher in *ppap-1* and *bg6-1* relative to wildtype roots treated with 50 μ M copper. These results indicate that copper levels are altered in the meristem of *bg_ppap-1* and *bg6-1* roots relative to wildtype. The region of the root with the most substantial increases in copper in the *bg_ppap-1* and *bg6-1* roots at 24 h is also the region of the root whose development appears most affected by excess copper at day 3. These results suggest that in the absence of *BG_PPAP* or *BG6* roots are less able to restrict copper from the root meristem perhaps due to reduced symplastic movement of copper in these lines.

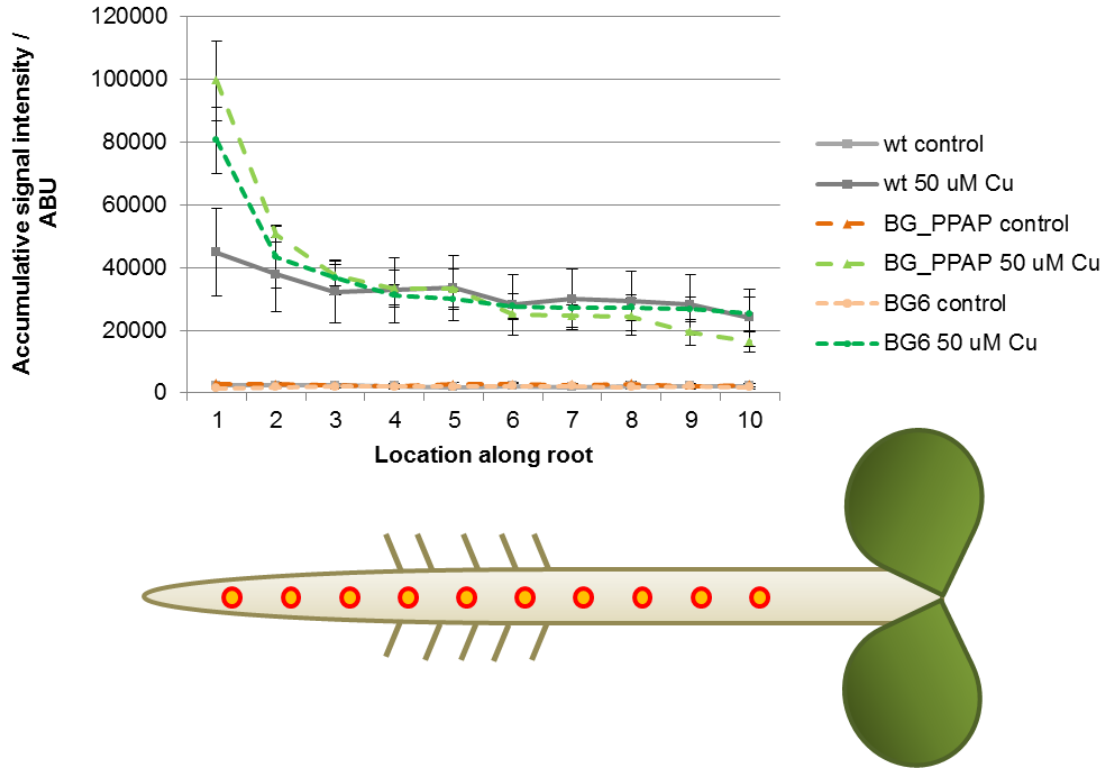


Figure 2.19 β -1,3-glucanase mutants accumulate excess copper in root tip compared to wildtype. Accumulative signal intensity in arbitrary units of copper levels in wildtype, *bg_ppap-1*, and *bg6-1* after 24 hours of 50 μ M Cu. X-axis corresponds to sample taken along the root, with punch 1 being at the meristem and moving shootwards.

3. CONCLUSIONS AND FUTURE DIRECTIONS

The focus of this work was to study how environmental stressors can affect plasmodesmata-mediated signaling. After exposure to seven different nutrient starvation and heavy metal excess conditions, we found that plasmodesmata closure in response to stress is not a universal response, as was previously thought. Upon investigating the deposition of callose in roots after exposure to stress, significant phenotypes were found in high iron (phloem-specific deposition) and high copper (callose breakdown) that correlated with the observed decrease and increase in symplastic signaling, respectively. Genetic analysis identified enzymes in the callose synthase and β -1,3-glucanase families, involved in callose deposition and breakdown, that were responsible for these callose-mediated modifications to plasmodesmata transport. We find that these regulated changes in plasmodesmata signaling in response to stress affect root growth, health, and mineral distribution. Most importantly, opening plasmodesmata under excess copper allows for better root growth, improved tolerance to copper, and reduced copper levels in the root meristem. This work contributes to our knowledge of plasmodesmata signaling during nutrient stress by identifying the genes and mechanisms that play a role in regulating intercellular signaling during high copper and iron stress, and by beginning to elucidate what the biological benefit might be to these modifications.

Symplastic isolation of the phloem in response to iron stress

Exposure to excess iron causes a fast and dramatic symplastic isolation of the phloem. This tissue specificity is confirmed by the RICS data, which show that plasmodesmata transport at the root tip remains normal under high iron. While not related to conditions of excess iron, symplastic isolation of the phloem is also observed during the normal potato tuber life cycle. In that system, symplastic gating plays a role in both tuber induction and dormancy break by controlling the allocation of resources to

meristematic or vegetative tissues (53). While the callose deposition in response to excess iron is dramatic, root cells are not dead (as shown by *cycb1;1*:GUS and propidium iodine staining) and plasmodesmata transport returns to normal after roots are removed from stress (as shown by SUC2:GFP diffusion recovery). This suggests that this is a biologically adaptive response, not the root responding by dying or entering dormancy. However, it is not clear what benefit (if any) there is to the deposition of phloem callose in response to excess iron.

One possibility is that this strong phloem block may serve to protect the meristem from excess iron accumulation. For iron to be distributed to the root organ, it is first sent up the xylem to the shoot, then loaded into the phloem for redistribution to sink tissues (22). We hypothesized that under high iron conditions, wildtype lines would have low levels of iron in the meristem, while the *CalS* mutants would have high iron accumulation, since they are unable to deposit phloem callose. However, we were unable to detect changes in iron accumulation in the root meristem using our LA-ICP-MS methods. The iron signal was very low in our mass spectrometry data, regardless of treatment condition or genotype. While this system is ideal for measuring many different elements, it is not very sensitive to detecting iron. Thus, we were unable to determine if ameliorating phloem callose leads to alterations in iron distribution in the root. However, if our hypothesis about protecting the meristem is correct, it may be that keeping that population of cells safe from toxic iron is a priority for the plant, even if this callose deposition correlates with inhibition of primary root growth (discussed later).

An alternative experimental approach would be to perform traditional ICP-MS (37), without the laser ablation. However, because of the amounts of dry tissue required for this technique, one would need thousands of *Arabidopsis* seedling roots for each

treatment. Additionally, because entire organs are ground up for processing, any spatial information about distribution within the root would be lost.

A more informative alternative approach would be to use synchrotron x-ray fluorescence (SXRF) to get *in vivo* metal abundance data without fixation or sectioning. Briefly, the SXRF technique involves exciting a sample with synchrotron x-rays, and capturing the emission based on an element's characteristic energy. This method provides spatial resolution in the sub- μm range, and sub- mg kg^{-1} detection sensitivity (106). The technique has been optimized for use in various plant tissues, including *Arabidopsis* roots, by the Guerinot lab, and more recently used in the Vatamaniuk lab (159) to analyze iron and copper levels in leaves.

Increasing plasmodesmatal permeability in response to copper stress

One of the most exciting results from this work was the finding that excess levels of copper induce an increase in plasmodesmata transport. With the exception of osmotic stress, all other biotic and abiotic stressors reported in the literature (pathogenesis, wounding, cold, metal toxicity) cause a decrease in plasmodesmata permeability. This led us to wonder why copper would have such a different effect on plasmodesmata compared to other metals like iron, and the finding that copper is particularly toxic among heavy metals. While land plants contain $140 \mu\text{g}$ of iron per g^{-1} dry weight, they contain only $4.15 \mu\text{g}$ of copper (91), creating a very low threshold for optimal copper amounts. In ryegrass and other plant species tested, the order of metal toxicity is $\text{Cu} > \text{Ni} > \text{Mn} > \text{Pb} > \text{Cd} > \text{Zn} > \text{Hg} > \text{Fe}$; this order matches the order of metallic-organic complexes stability (147). Additionally, unlike iron, which can be safely bound to ferritin as a storage mechanism, copper has no similar mechanism (108). This increased toxicity particular to copper led us to the hypothesis that excess copper concentrations

would require a spreading of copper throughout the root to dilute levels in individual cells.

Our LA-ICP-MS experiments show that opening plasmodesmata under conditions of high copper results in reduced copper concentrations in the root meristem. This increase in plasmodesmata permeability appears to be beneficial to the plant; when this response is attenuated, plants have poorer root growth, increased sensitivity to copper stress, more severe developmental effects, and increased copper accumulation in the meristem. Given that heavy metals are presumed to move symplastically at several points in their long-distance transport, these findings highlight the importance of plasmodesmata-mediated transport of copper for appropriate distribution under conditions of excess.

An intriguing additional possibility is that opening plasmodesmata allows for the spreading of a signal necessary in the high copper response. In the case of phosphate starvation, for example, the long-distance transport of miR399 from the shoot to root is necessary for the expression of high affinity transporters to increase phosphate uptake (66, 99). In another example, the antiviral RNA silencing response during pathogenesis requires the spreading of small RNAs via plasmodesmata (105). Therefore; it is possible that a mobile signal needs to move via plasmodesmata under high copper stress as well. SPL7 has been proposed as the sensor for copper levels, activating copper chaperone CCH, copper transporters, and miR398 (which degrades proteins that require copper as a co-factor) under copper deficiency (154). However, under high copper conditions, SPL7 needs to be turned off. Regulation of SPL7 under high copper may involve degradation of the SPL7 protein, or inactivation by an as-yet unidentified copper-sensing protein, as proposed by Yamasaki, *et al.* (154). While we understand many of the steps involved in the copper deficiency response, the signaling pathway and regulators in

response to copper excess are still not clearly elucidated. It is possible that increasing plasmodesmata permeability may assist in the spreading of an unknown copper-sensing protein, thus allowing a signal to reach the meristem and instruct the root to cease copper uptake.

The role of CalS and β -1,3-glucanase enzymes in responding to specific environmental cues

Although callose is the best-studied regulator of plasmodesmata permeability, the field is still actively working to elucidate how CalS and β -1,3-glucanase enzymes respond to specific cues to regulate callose metabolism. A recent 2014 review listed all of the known callose synthases and β -1,3-glucanases that influence plasmodesmata permeability through callose turnover (30); there were only three of each kind. The current work contributes to that list and supports previous findings that there may be subfunctionalization of the CALS genes. We found that of the genes tested, only CalS12 acts in the iron stress response. While we did not screen all 50 β -1,3-glucanase genes under high copper, single mutants for *BG_PPAP* and *BG6* were enough to significantly impact how roots respond to this stress. Therefore, even though this is a large family, there may be specificity between genes and signals. The other 48 genes do not appear to compensate, suggesting there is less genetic redundancy than we may have expected.

Moving forward, it will be valuable to understand more about how these enzymes are regulated. Correlative studies have shown that calcium and ROS signaling are linked to activation of CalS enzymes (discussed further below). However, we still do not know how these signals are integrated at plasmodesmata and transmitted to the CalS complex. Even less is known about the regulation of the β -1,3-glucanase enzymes. The

class D β -1,3-glucanase genes, which we screened in this study, are transcriptionally regulated in response to hormone treatment, ozone stress, and bacterial or pathogen infection, as determined by microarray expression data (34). However, the upstream regulators and signaling components are still unidentified. Learning more about the regulation and activation of these enzymes will contribute to our understanding of the steps in turning an environmental cue into a modification of intercellular signaling.

One promising avenue of inquiry would be the relationship between the plasmodesmata-localized proteins (PDLPs) and callose synthases. PDLPs were identified in a plasmodesmata proteome study (41), and confirmed via microscopy to localize to plasmodesmata (75). In salicylic acid-dependent defense responses, PDLP5 is required for appropriate plasmodesmata closure, and PDLP5 overexpresser lines have four times higher callose levels at plasmodesmata than wildtype. However, the precise function of PDLPs is still unknown, and how exactly they contribute to callose deposition is unclear, since they have no callose synthesis activity of their own. It is likely that the PDLPs work to activate the callose synthase enzymes at plasmodesmata through a still-unknown mechanism.

The link between callose deposition and primary root growth

For some time, scientists in the field have been interested in definitively concluding if the deposition of callose causes inhibition of primary root growth. A study using the callose synthesis inhibitor 2-deoxy-D-glucose in wheat cultivars found that inhibition of callose synthesis rescues primary root growth of wheat roots exposed to aluminum toxicity (127). However, 2-deoxy-D-glucose can also inhibit cellulose synthesis, so these effects are not callose-specific. Another more recent study found that overproduction of callose led to inhibition of primary root growth (139). In this study, an estradiol-inducible

system was used to activate the *icals3m* construct, expressing a gain-of-function CALS3, which led to excess callose levels and significantly shorter roots than wildtype.

Here we were able to assess the effects of callose deposition on root growth using mutant analysis. Under normal conditions, the β -1,3-glucanase mutants *bg_ppap* and *bg6* have higher callose levels than wildtype, and after exposure to high copper stress, do not decrease callose levels in the root. These mutants also grow more poorly under high copper stress than wildtype, showing an increased inhibition of primary root growth. The callose synthase mutant *cal5* has equal levels of callose as wildtype under normal conditions, and a similar inhibition of primary root growth as wildtype under high iron stress. Conversely, *cal12* has significantly lower callose levels than wildtype under control conditions, and shows much less primary root growth inhibition in response to high iron (43% compared to 72%). High zinc, which elicits no obvious changes in callose deposition, also elicits no inhibition of primary root growth, in wildtype or mutant lines, after 1 or 3 days.

The strongest support for the model of callose driving root growth inhibition in this work comes from the growth assays of *bg_ppap* and *bg6* on high iron, and *cal2* and *cal12* on high copper. The β -1,3-glucanase mutants, which have higher overall levels of callose, also have more severe primary root growth on high iron than *cal5*, which has the lowest callose levels. Under high copper, *cal5*, which has the lowest basal callose levels, also shows the least inhibition of primary root growth. *cal12*, which has similar callose levels as wildtype, shows similar primary root growth inhibition (27% and 29%, respectively).

Our results are consistent with recent findings in a recent 2015 study by Zhang, *et al.* (160). This group screened 71 cultivars of sweet sorghum for aluminum tolerance. They found that the aluminum-tolerant ROMA cultivar also had lower callose synthase activity,

higher β -1,3-glucanase activity, and reduced callose accumulation after 24 hours of aluminum exposure. Conversely, the most aluminum-sensitive cultivar, POTCHETSTRM, had higher callose synthase activity, lower β -1,3-glucanase activity, and accumulated more callose in root apices in response to aluminum treatment. Interestingly, when the β -1,3-glucanase responsible for these differences, SbGlu1, was heterologously expressed in *Arabidopsis*, these plants also showed reduced callose accumulation and greater aluminum tolerance, as assayed by primary root growth. Thus, under either excess aluminum or copper, a decrease in callose levels in the root correlates with improved root growth.

Why would plants increase callose deposition if it stunts root growth? One possibility is that this allows for the loss of apical dominance, and an increasingly branched root system. Under suboptimal nutrient conditions, root system architecture changes to deploy more lateral roots at the expense of primary root growth. This is thought to increase foraging capacity for a more optimal nutrient patch. Classic experiments using barley grown in soils with heterogeneously distributed nutrients show that the root system has dramatically increased lateral roots and root hairs only in the zone of nutrient stress (112). Thus, stress does not cause a complete cessation of growth, but rather a redistribution of growth.

Determining the mechanism of plasmodesmata regulation under zinc stress

After exposure to excess or deficient zinc, *Arabidopsis* roots show changes in plasmodesmata transport that appear to be independent of callose accumulation (in contrast to what was observed with high copper and iron). Even when zinc levels were increased to 500 μ M, or the exposure time was increased to 7 days, no changes in callose were observed. One possibility is that callose levels are changing at a range that

is undetectable with aniline blue imaging. Aniline blue is as fast as an inexpensive technique; however, there may be high background levels due to non-specific staining (157). Immuno-labeling of callose gives more sensitive and cleaner images, but is labor-intensive due to the fixation and sectioning required (101). To confidently rule out callose changes during high zinc stress, future experiments could use commercially available antibodies to perform immuno-labeling of callose under these conditions.

An alternate possibility is that the changes in plasmodesmata transport under zinc stress are callose-independent. Some support for this is the finding that excess zinc has no effect on primary root growth (discussed above). While callose is the best understood regulator of plasmodesmata permeability, other molecules, subcellular domains, and structural differences can regulate cell-cell connectivity. Changes in plasmodesmata structure, microdomains, or membrane contact sites (MCS) all influence plasmodesmata permeability. These are all plasmodesmata alterations we would not detect with our aniline blue staining experiments under zinc stress. One possibility that was preliminarily investigated in this work was whether there are changes in the frequency and structure of plasmodesmata under high zinc conditions. Using cryo-EM techniques of high pressure freeze and freeze substitution (15), longitudinal ultra-thin sections of the root tip were prepared for TEM imaging. Due to the laborious and expensive nature of the sample preparation, and the time-intensive process of quantifying plasmodesmata numbers using TEM, this avenue of research was not pursued further, but future work may use this preliminary data for further exploration.

Another feature of zinc stress is that while there is an increase of CF movement shootwards in both high and low zinc, there is either a decrease (low zinc), or no significant changes in GFP movement (high zinc) out of the phloem. One possibility for this is that we are using two fluorescent molecules of different sizes (GFP is 27 kDa,

while CFDA is much smaller at ~1 kDa), and we are observing increased allowance of CF movement, but not necessarily GFP. Alternatively, because we observed different changes in plasmodesmata transport between directions (outwards from the phloem compared to from root to shoot), it is possible that the phloem and stele tissues may experience different modifications to plasmodesmata permeability than the ground tissues and epidermis do. Other stresses like salt and low iron elicit tissue-specific transcriptional responses (32). Perhaps in the case of zinc, there are tissue-specific transcriptional events that culminate in different regulation of intercellular signaling. Nothing is known yet about tissue-specific responses to excess zinc, but to determine this, future work could perform Fluorescence Activated Cell Sorting (FACS) to look at the transcriptional profiles of different cell types after exposure to zinc stress (13, 16).

The role of ROS in heavy metal stress

While excessive and prolonged exposure to ROS results in cell death, ROS is also an important upstream signaling component in stress responses. Literature in the field about ROS localization and production is controversial. For example, while some groups have documented that excess zinc leads to increased ROS, others have found that this is only the case in mutants lacking vacuolar sequestration (64). Part of the difficulty in studying ROS is the rapid kinetics of ROS production, the involvement in all steps of the stress response (signal perception, transduction, and amplification), the difficulty in reliably detecting levels and localization, and the crosstalk between ROS and hormones and nitric oxides. Additionally, preliminary data in my thesis (unpublished) found that mutants in ROS production fail to make phloem callose under high iron stress, supporting the body of work linking ROS signaling to stress responses. In this work, the

role of ROS in influencing root growth, activating CalS enzymes, and regulating plasmodesmata permeability is of particular interest.

The balance of types of ROS molecules has been shown by Tsukagoshi, *et al.*, to regulate the switch between cell proliferation and differentiation (137). The transcription factor UPBEAT1 (UPB1) regulates the expression of three peroxidase genes that in turn regulate the levels of superoxide and hydrogen peroxide in specific root zones. These opposing gradients of superoxide and hydrogen peroxide control the transition between division at the meristem and differentiation at the transition zone in the root. Interestingly, based on observed differences between the localization of UPB1 mRNA and protein, UPB1 may move from the lateral root cap to the elongation zone. Because excess copper and iron induce ROS accumulation, inhibition of primary root growth, and changes in plasmodesmata permeability, it would be interesting to determine the role of UPB1 in the root responses observed under copper and iron stress. If UPB1 requires plasmodesmata for its intercellular movement, one could study how high copper or iron changes UPB1 distribution, and if this correlates with change in primary root growth under these conditions.

As stated above, very little is known about how signals are integrated at the plasmodesmata to activate CalS enzymes. However, studies have shown a correlation between ROS production and callose deposition in both developmental processes (pollen development, elongation of cotton fibers, stomata patterning, and transition to senescence) and stress responses (viral infection, aluminum and cadmium exposure). Additionally, forward genetic screens for mutants in symplastic transport have mostly yielded mutations in genes involved in redox homeostasis. Mutants in GFP-ARRESTED TRAFFICKING (GAT1), have defects in the plastid thioredoxin TRX-m3, which is an enzyme responsible for protein redox activation and inactivation. *gat1* mutants show an

increased accumulation of both callose and ROS (9). Conversely, mutants in INCREASED SIZE EXCLUSION LIMIT 1 (ISE1), which have defects in a mitochondrial RNA helicase, have increased intercellular transport, though still accompanied by increased ROS levels (131). These two mutants both have increased ROS, but different effects on plasmodesmata permeability. The plastid and mitochondria make different ROS intermediates and in different concentrations, therefore the subcellular origin, ROS amount, and ROS type may activate different signaling pathways that lead to different plasmodesmata modifications.

Because high copper increases ROS levels, but we see an increase in plasmodesmata permeability, it is likely that ROS is being produced from the mitochondria, resulting in plasmodesmata widening. To test this hypothesis, future work could utilize the organelle-targeted ROS sensors developed in the Zambryski lab to determine the redox state of subcellular compartments, and confirm if the mitochondria is responsible for the ROS production under high copper stress (130). These sensors consist of GFP variants, target to either the cytoplasm (cyto-roGFP1), plastid (plastid-roGFP2), or mitochondria (mito-roGFP1). Importantly, two cysteine residues have been introduced near the fluorophore, allowing for the formation of a disulfide bond dependent on the redox state of the organelle. The different conformations of the fluorophore have different peak fluorescence excitation wavelengths (400nm in neutral form, 495nm in anionic form), which can then be detected via confocal microscopy.

In summary, this work has contributed to our knowledge of how plants regulate intercellular signaling in response to environmental challenges. Callose, the best-studied regulator of plasmodesmata permeability, modifies plasmodesmata transport under excess copper or iron, although we cannot rule out its role in stresses that fail to show

obvious changes in callose localization or levels. Elucidating the genes responsible for regulating these modifications contributes to what we know about callose synthase and β -1,3-glucanase enzymes, and their roles in responding to specific cues. Most importantly, plasmodesmata modifications under heavy metal stress have significant impacts on plant health and survival. Altering the plant's normal plasmodesmata responses affects root growth, cellular morphology, and mineral distribution under heavy metal stress.

While plasmodesmata have been studied for over 138 years, the field at this time is actively trying to further understand mechanisms of regulation in this important signaling pathway. At this juncture, there are many possible avenues to pursue. Future work should focus on continuing to identify specific roles for proteins that regulate callose turnover at plasmodesmata, better understanding callose-independent mechanisms of intercellular transport regulation, elucidating the role of ROS in root responses to excess heavy metals, and discovering if mobile signals are being propagated via plasmodesmata under high copper stress.

Outside of basic science, the findings from this work have potential for biotech applications as well. Many applied and translational groups are working on exploiting adaptive responses to create better crops and agricultural products. As global populations continue to rise and the changing climate threaten our food security, maximizing crop production efficiency will continue to be of interest.

4. MATERIALS AND METHODS

Plant Material and Growth Conditions

A. thaliana wildtype ecotype Col-0 was used along with mutant lines (Supplemental table 1). *Cycb1;1:GUS* lines were provided by Dr. Scott Poethig, University of Pennsylvania. *SUC2:GFP* lines were provided by Dr. Stefan Abel, University of California, Davis. *CalS* lines (as indicated in Table 4.1) were provided by Dr. Jung-Youn Lee, University of Delaware. All seeds were sterilized using 20% bleach solution, and kept in 4°C for 2 days before sowing onto 1x MS plates with 5% sucrose and 5% Difco Agar. Plants were grown in incubation chamber using 16-hr light / 8-hr dark cycle at 23°C. After 5 days, seedlings were transferred to stress media for 1 or 3 days (indicated in text) before analyzing. For plates containing excess heavy metals, the following concentrations were added to 1xMS media: 50 µM CuSO₄, 150 µM ZnSO₄, 600 µM FeEDTA, or 85 µM CdCl₂. For low nutrient plates, media was made with the following concentrations of macro and micronutrients (instead of using MS): 5 mM potassium nitrate, 2 mM calcium nitrate, 2 mM magnesium sulfate, 2.5 mM potassium phosphate, 14 µM manganese chloride, 70 µM boric acid, 1 µM zinc sulfate, 0.5 µM copper sulfate, 0.2 µM sodium molybdate, 0.01 µM cobalt chloride, and 50 µM NaFe EDTA. For low phosphate media, potassium phosphate was omitted, 2.5 mM potassium chloride added as a potassium source, and washed agar was also used. For low iron media, NaFe EDTA was omitted, and 100 µM Ferrozine (an iron chelator) was added. For low zinc media, ZnSO₄ was omitted from the media.

Table 4.1 Germplasm used in this study

Gene	Allele	Line	Reference	Source
CalS1	<i>cals1-1</i>	SALK_142792	Weier et al., 2016	Jung-Youn Lee, UDel
CalS2	<i>cals2-1</i>	SAIL_1276_E05	Weier et al., 2016	Jung-Youn Lee, UDel
CalS3	<i>cals3-5</i>	SALK_068418	Vaten et al., 2011	Jung-Youn Lee, UDel
CalS4	<i>cals4-1</i>	SALK_009569	this study	ABRC
CalS5	<i>cals5-2</i>	SALK_026354	Dong et al., 2005	ABRC
CalS5	<i>cals5-3</i>	CS68974	Nishiwaka et al., 2005	ABRC
CalS5	<i>cals5-5</i>	SALK_072226	Nishiwaka et al., 2005	ABRC
CalS6	<i>cals6-1</i>	FLAG_335D06	Weier et al., 2016	ABRC
CalS7	<i>cals7-1</i>	SALK_048921	Xie et al., 2011	Jung-Youn Lee, UDel
CalS8	<i>cals8-1</i>	SALK_037603	this study	ABRC
CalS11	<i>cals11-1</i>	SAIL_18_G03	Weier et al., 2016	ABRC
CalS12	<i>cals12-1/pmr4-1</i>	CS3858	Nishimura et al., 2003	Jung-Youn Lee, UDel
CalS12	<i>cals12-2/pmr4-5</i>	CS67146	Nishimura et al., 2003	ABRC
At BG_PPAP	<i>bg_ppap-1</i>	SALK_019116	Levy et al., 2007	ABRC
At BG_PPAP	<i>bg_ppap-2</i>	SAIL_115_G04	Levy et al., 2007	ABRC
At4g16260	<i>bg6-1</i>	SALK_031479	this study	ABRC
At4g16260	<i>bg6-2</i>	SAIL_1280_B05	this study	ABRC
At1g30080	<i>bg7</i>	SALK_078006	this study	ABRC
At4g18340	<i>bg8</i>	SALK_053553	this study	ABRC

Table 4.2 Primers used in this study

Primers used in Semi-qRT-PCR		
	Primer Name	5`-3`
EIF4a	Forward primer	AAACTCAATGAAGTACTTGAGGGACA
	Reverse primer	TCTCAAAACCATAAGCATAAATACCC
cals4-1	Forward primer	GCTAACGGAAGTGGTGAGCA
	Reverse primer	TAAAGGCGCTGAGTTGATACACA
cals8-1	Forward primer	GGAGATGGCGAGGAATGCTT
	Reverse primer	GGTCAGGAGAACCAGAATCCAG
bg6-1	Forward primer	TCACAACCATCCTCAACCCAA
	Reverse primer	AGCGTTCAACGGCAGAGTAA
bg6-2	Forward primer	TCACAACCATCCTCAACCCAA
	Reverse primer	AGCGTTCAACGGCAGAGTAA
bg7	Forward primer	ACCAAGATCGGTGGTATCGC
	Reverse primer	TCTTTAAAGCCGTGGAGGCA
bg8	Forward primer	AACGAGCTTTTCACCGACGA
	Reverse primer	TCCTCTTTGCCTTAGTGGCAG

Primers Used in Genotyping		
Allele	Primer Name	5`-3`
cals1-1	Left primer	CTATGTCTTGCCTTCCAGCTG
	Right primer	GCTTTCCTGCAGAAAGTTGTG
cals2-1	Left primer	CCCTTTTTCTTTGGAGTTTCG
	Right primer	CTCTCTACATTGCTCTTCGCG
cals3-5	Left primer	AGCTCCAAGGCTTTTCGATAG
	Right primer	AGATTCAAGTCATGGTGGCAC
cals4-1	Left primer	GACAATAGCCGAGGTTGTTTG
	Right primer	AATATAAGCCCGCGGTATACC
cals5-2	Left primer	ACCTCTCCCAAACGATCAAAG
	Right primer	TCATTTTTCCAATGCTTCGAC
cals5-3	Left primer	GTGTACCAATTGAACTTACC
	Right primer	CTTACCACCGGCGAGAATACG
cals5-5	Left primer	CCAGATTCCGGTTTTCTTTC
	Right primer	TGTGGATTTCTCCATCGGTAG
cals6-1	Left primer	GTGACTTGATTCAGCCTCTGC
	Right primer	ACCGTCACTGAGTTGATGGAC
cals7-1	Left primer	TGGCAAGAATAGATCCTGACG
	Right primer	ATGGATGGTTTTCTATTGGC
cals8-1	Left primer	TTCGTTCCACGTCCTTGTATC
	Right primer	TCTGTGAAGGATTGAACAGGC
cals11-1	Left primer	CATTCATGAGCACACCATCAC
	Right primer	CAACATAGAGAAGCTCACGGC
cals12-1	Left primer	ATCAGGTGCGAGGCCAACAAG
	Right primer	CACCCGCCCACTATCTGTTT
cals12-2	Left primer	GATCGACTTTGGGTGATGC
	Right primer	CACTAAACCCTCTCTCAAACC
bg_ppap-1	Left primer	TGA TCC CAA GTG AGT AAA CCG
	Right primer	TGC TCA CAA CCA CTC ACT ACG
bg_ppap-2	Left primer	AGGTCGCTAACAACCTTCCTC
	Right primer	GTAATCCGGTGATGGGTTACC
bg6-1	Left primer	AACTCTTCCCTCCTTCCTCC
	Right primer	TGAATTATCACCGTCGCTAGC
bg6-2	Left primer	AGTCTCGCGTCGACAGTGTAC
	Right primer	ACGTTGTTTACTCTGCCGTTG
bg7	Left primer	AGTGGGCAATTCAATTTTTCC
	Right primer	AGGCTTGAGTCATCGTCAGTG
bg8	Left primer	CGTCTTTTTCTCCATGATTATCG

	Right primer	TTCCCAACTTGTCCGTAATTG
--	--------------	-----------------------

Growth measurements

5 day old seedlings were transferred to indicated stress media for 1 or 3 days (indicated in text). Growth of primary root during stress exposure was measured using Image J segmented line function. 2-tailed t-test, $p < 0.05$.

Aniline blue staining

Seedlings were stained in aniline blue solution (750 μ l 67 mM K_3PO_4 pH 9.5, 240 μ l distilled water, 1 μ l Silwet-77, and 10 μ l 1% aniline blue) in the dark for 1 hour prior to imaging. Images were taken using a Leica SP5 scanning confocal microscope using a 405 laser. When quantified, entire root was selected as a region of interest and mean fluorescence intensity was measured using ImageJ.

GUS staining

Entire seedlings were placed in ice-cold 90% acetone or 10 minutes. Acetone was then removed and replaced with staining buffer containing 50mM PO_4 buffer, 0.2% Triton-X, 2mM ferrocyanide/ferricyanide, and incubated for 10 minutes. Staining buffer was then removed and replaced with staining buffer containing 2mM X-Gluc and incubated for 15 minutes. Samples were incubated at 37 °C overnight. Samples were then washed three times with 70% ethanol, and imaged using DIC.

CFDA

5(6)-Carboxyfluorescein diacetate (CFDA) was dissolved in dimethyl sulfoxide at 50mM stock concentration and stored at -20°C. Fresh working solution was prepared for each

experiment by diluting the stock 1:50 in autoclaved water. 2 μ l of working solution CFDA was applied to root tips and incubated at room temperature for 5 minutes. Roots were imaged on a fluorescent dissecting microscope using GFP filter. The extent of CF movement from root tip towards shoot was measured using Image J segmented line function. Color threshold was adjusted to include only strong green signal, and exclude dim signals and autofluorescence. Wilcoxon rank sum test, $p < 0.05$. Boxplot created using R Studio.

SUC2:GFP

5 day old SUC2:GFP seedlings were transferred to stress media for 1 day. Roots were then imaged using Leica SP5 confocal microscope using a 488 laser. Propidium Iodide was used as a counter stain for the cell wall. Ratiometric data was generated by taking phloem:meristem fluorescence intensity ratios. Fluorescent profiles were generated by drawing a transverse line across the width of the root and using ImageJ's plot profile feature.

RICS

5 day old 35S::GFP seedlings were transferred to stress media for 24 hours. Raster Image Correlation Spectroscopy (RICS) performed according to Clark, et al, 2016 (21). Images were collected using a Zeiss 710 confocal microscope. For Raster Image Correlation Spectroscopy, frames were acquired using Raster scan with a dwell time of 12.61 μ sec / pixel, for 100 frame series. Diffusion coefficient was derived using SimFCS software's autocorrelation function. Wilcoxon rank sum test, $p < 0.05$. Boxplot created using R Studio.

LA-ICP-MS

Laser ablation- inductively coupled plasma – mass spectroscopy performed according to Shimotohno, et al, 2015 (124). After 24 hours of metal stress, live *Arabidopsis* seedlings were mounted on microscope slides using double sided tape. Positions for laser ablation were set using computer software and camera, with a spot size of 10 μ M and a spacing of 30 μ M between punches.

BIBLIOGRAPHY

1. Amor Y, Haigler CH, Johnson S, Wainscott M, & Delmer DP (1995) A membrane-associated form of sucrose synthase and its potential role in synthesis of cellulose and callose in plants. *Proceedings of the National Academy of Sciences* 92(20):9353-9357.
2. Anderson MA, *et al.* (1991) Long-term effects of copper rich swine manure application on continuous corn production. *Communications in Soil Science & Plant Analysis* 22(9-10):993-1002.
3. Andrawis A, Solomon M, & Delmer DP (1993) Cotton fiber annexins: a potential role in the regulation of callose synthase. *The Plant Journal* 3(6):763-772.
4. Andrés-Colás N, *et al.* (2006) The Arabidopsis heavy metal P-type ATPase HMA5 interacts with metallochaperones and functions in copper detoxification of roots. *The Plant Journal* 45(2):225-236.
5. ANGELL SM, DAVIES C, & BAULCOMBE DC (1996) Cell-to-cell movement of potato virus X is associated with a change in the size-exclusion limit of plasmodesmata in trichome cells of *Nicotiana clevelandii*. *Virology* 216(1):197-201.
6. Arias M, López E, Fernández D, & Soto B (2004) Copper distribution and dynamics in acid vineyard soils treated with copper-based fungicides. *Soil science* 169(11):796-805.
7. Bais HP, Weir TL, Perry LG, Gilroy S, & Vivanco JM (2006) The role of root exudates in rhizosphere interactions with plants and other organisms. *Annu. Rev. Plant Biol.* 57:233-266.
8. Barclay GF, Peterson CA, & Tyree MT (1982) Transport of fluorescein in trichomes of *Lycopersicon esculentum*. *Canadian Journal of Botany* 60(4):397-402.
9. Benitez-Alfonso Y, *et al.* (2009) Control of Arabidopsis meristem development by thioredoxin-dependent regulation of intercellular transport. *Proceedings of the National Academy of Sciences* 106(9):3615-3620.
10. Benitez-Alfonso Y, *et al.* (2013) Symplastic intercellular connectivity regulates lateral root patterning. *Developmental cell* 26(2):136-147.
11. Benitez-Alfonso Y, Jackson D, & Maule A (2011) Redox regulation of intercellular transport. *Protoplasma* 248(1):131-140.
12. Bi Y, *et al.* (2009) Production of reactive oxygen species, impairment of photosynthetic function and dynamic changes in mitochondria are early events in cadmium-induced cell death in Arabidopsis thaliana. *Biology of the Cell* 101(11):629-643.
13. Birnbaum K, *et al.* (2005) Cell type-specific expression profiling in plants via cell sorting of protoplasts from fluorescent reporter lines. *Nature methods* 2(8):615-619.
14. Blamey FP, Joyce D, Edwards D, & Asher C (1986) Role of trichomes in sunflower tolerance to manganese toxicity. *Plant and Soil* 91(2):171-180.
15. Bobik K, Dunlap JR, & Burch-Smith TM (2014) Tandem high-pressure freezing and quick freeze substitution of plant tissues for transmission electron microscopy. *Journal of visualized experiments: JoVE* (92).
16. Bonner W, Hulett H, Sweet R, & Herzenberg L (2003) Fluorescence activated cell sorting. *Review of Scientific Instruments* 43(3):404-409.

17. Cantrill L, Overall R, & Goodwin P (1999) CELL-TO-CELL COMMUNICATION VIA PLANT ENDOMEMBRANES. *Cell biology international* 23(10):653-661.
18. Carella P, Isaacs M, & Cameron R (2015) Plasmodesmata-located protein overexpression negatively impacts the manifestation of systemic acquired resistance and the long-distance movement of Defective in Induced Resistance1 in Arabidopsis. *Plant Biology* 17(2):395-401.
19. Carlsbecker A, *et al.* (2010) Cell signalling by microRNA165/6 directs gene dose-dependent root cell fate. *Nature* 465(7296):316-321.
20. Chang C-L, *et al.* (2013) Feedback regulation of receptor-induced Ca²⁺ signaling mediated by E-Syt1 and Nir2 at endoplasmic reticulum-plasma membrane junctions. *Cell reports* 5(3):813-825.
21. Clark NM, *et al.* (2016) Tracking transcription factor mobility and interaction in Arabidopsis roots with fluorescence correlation spectroscopy. *Elife* 5:e14770.
22. Clemens S, Palmgren MG, & Krämer U (2002) A long way ahead: understanding and engineering plant metal accumulation. *Trends in plant science* 7(7):309-315.
23. Cohen CK, Norvell WA, & Kochian LV (1997) Induction of the root cell plasma membrane ferric reductase (an exclusive role for Fe and Cu). *Plant Physiology* 114(3):1061-1069.
24. Cole LJ, McCracken DI, Foster GN, & Aitken MN (2001) Using Collembola to assess the risks of applying metal-rich sewage sludge to agricultural land in western Scotland. *Agriculture, ecosystems & environment* 83(1):177-189.
25. Corbesier L, *et al.* (2007) FT protein movement contributes to long-distance signaling in floral induction of Arabidopsis. *science* 316(5827):1030-1033.
26. Cosgrove DJ (2005) Growth of the plant cell wall. *Nature reviews. Molecular cell biology* 6(11):850.
27. Crawford KM & Zambryski PC (2001) Non-targeted and targeted protein movement through plasmodesmata in leaves in different developmental and physiological states. *Plant Physiology* 125(4):1802-1812.
28. Cui W & Lee J-Y (2016) Arabidopsis callose synthases CalS1/8 regulate plasmodesmal permeability during stress. *Nature plants* 2:16034.
29. Cuypers A, *et al.* (2012) Cadmium and copper stress induce a cellular oxidative challenge leading to damage versus signalling. *Metal Toxicity in Plants: Perception, Signaling and Remediation*, (Springer), pp 65-90.
30. De Storme N & Geelen D (2014) Callose homeostasis at plasmodesmata: molecular regulators and developmental relevance. *Specialised membrane domains of plasmodesmata, plant intercellular nanopores*:94.
31. Deom CM, Lapidot M, & Beachy RN (1992) Plant virus movement proteins. *Cell* 69(2):221-224.
32. Dinneny JR, *et al.* (2008) Cell identity mediates the response of Arabidopsis roots to abiotic stress. *Science* 320(5878):942-945.
33. Dong X, Hong Z, Sivaramakrishnan M, Mahfouz M, & Verma DPS (2005) Callose synthase (CalS5) is required for exine formation during microgametogenesis and for pollen viability in Arabidopsis. *The Plant Journal* 42(3):315-328.
34. Doxey AC, Yaish MW, Moffatt BA, Griffith M, & McConkey BJ (2007) Functional divergence in the Arabidopsis β -1, 3-glucanase gene family inferred by phylogenetic reconstruction of expression states. *Molecular biology and evolution* 24(4):1045-1055.

35. Duckett CM, Oparka KJ, Prior DA, Dolan L, & Roberts K (1994) Dye-coupling in the root epidermis of Arabidopsis is progressively reduced during development. *Development* 120(11):3247-3255.
36. Enns LC, *et al.* (2005) Two callose synthases, GSL1 and GSL5, play an essential and redundant role in plant and pollen development and in fertility. *Plant molecular biology* 58(3):333-349.
37. Fassel VA & Kniseley RN (1974) Inductively coupled plasma. Optical emission spectroscopy. *Analytical Chemistry* 46(13):1110A-1120a.
38. Faulkner C, Akman OE, Bell K, Jeffree C, & Oparka K (2008) Peeking into pit fields: a multiple twinning model of secondary plasmodesmata formation in tobacco. *The Plant Cell* 20(6):1504-1518.
39. Faulkner C, *et al.* (2013) LYM2-dependent chitin perception limits molecular flux via plasmodesmata. *Proceedings of the National Academy of Sciences* 110(22):9166-9170.
40. Feng G, *et al.* (2002) Improved tolerance of maize plants to salt stress by arbuscular mycorrhiza is related to higher accumulation of soluble sugars in roots. *Mycorrhiza* 12(4):185-190.
41. Fernandez-Calvino L, *et al.* (2011) Arabidopsis plasmodesmal proteome. *PLoS One* 6(4):e18880.
42. Fisher DB (1999) The estimated pore diameter for plasmodesmal channels in the Abutilon nectary trichome should be about 4 nm, rather than 3 nm. *Planta* 208(2):299-300.
43. Foley RC & Singh KB (1994) Isolation of a Vicia faba metallothionein-like gene: expression in foliar trichomes. *Plant molecular biology* 26(1):435-444.
44. Foyer CH & Noctor G (2009) Redox regulation in photosynthetic organisms: signaling, acclimation, and practical implications. *Antioxidants & redox signaling* 11(4):861-905.
45. Gimenez-Ibanez S, Ntoukakis V, & Rathjen JP (2009) The LysM receptor kinase CERK1 mediates bacterial perception in Arabidopsis. *Plant signaling & behavior* 4(6):539-541.
46. Gisel A, Barella S, Hempel FD, & Zambryski PC (1999) Temporal and spatial regulation of symplastic trafficking during development in Arabidopsis thaliana apices. *Development* 126(9):1879-1889.
47. Gisel A, Hempel FD, Barella S, & Zambryski P (2002) Leaf-to-shoot apex movement of symplastic tracer is restricted coincident with flowering in Arabidopsis. *Proceedings of the National Academy of Sciences* 99(3):1713-1717.
48. Gitan RS, Luo H, Rodgers J, Broderius M, & Eide D (1998) Zinc-induced inactivation of the yeast ZRT1 zinc transporter occurs through endocytosis and vacuolar degradation. *Journal of Biological Chemistry* 273(44):28617-28624.
49. Grabski S, De Feijter AW, & Schindler M (1993) Endoplasmic reticulum forms a dynamic continuum for lipid diffusion between contiguous soybean root cells. *The Plant Cell* 5(1):25-38.
50. Grison MS, *et al.* (2015) Specific Membrane Lipid Composition Is Important for Plasmodesmata Function in Arabidopsis. *The Plant Cell* 27(4):1228-1250.
51. Grotz N, *et al.* (1998) Identification of a family of zinc transporter genes from Arabidopsis that respond to zinc deficiency. *Proceedings of the National Academy of Sciences* 95(12):7220-7224.
52. Hall J (2002) Cellular mechanisms for heavy metal detoxification and tolerance. *Journal of experimental botany* 53(366):1-11.

53. Hancock RD, Roberts AG, & Viola R (2008) A role for symplastic gating in the control of the potato tuber life cycle. *Plant signaling & behavior* 3(1):27-29.
54. Helle SC, *et al.* (2013) Organization and function of membrane contact sites. *Biochimica et Biophysica Acta (BBA)-Molecular Cell Research* 1833(11):2526-2541.
55. Henne WM, Liou J, & Emr SD (2015) Molecular mechanisms of inter-organelle ER–PM contact sites. *Current opinion in cell biology* 35:123-130.
56. Holdaway-Clarke TL, Walker NA, Hepler PK, & Overall RL (2000) Physiological elevations in cytoplasmic free calcium by cold or ion injection result in transient closure of higher plant plasmodesmata. *Planta* 210(2):329-335.
57. Holmgren G, Meyer M, Chaney R, & Daniels R (1993) Cadmium, lead, zinc, copper, and nickel in agricultural soils of the United States of America. *Journal of environmental quality* 22(2):335-348.
58. Hong Z, Zhang Z, Olson JM, & Verma DPS (2001) A novel UDP-glucose transferase is part of the callose synthase complex and interacts with phragmoplastin at the forming cell plate. *The Plant Cell* 13(4):769-779.
59. Huang L, *et al.* (2009) Arabidopsis glucan synthase-like 10 functions in male gametogenesis. *Journal of plant physiology* 166(4):344-352.
60. Hussain D, *et al.* (2004) P-type ATPase heavy metal transporters with roles in essential zinc homeostasis in Arabidopsis. *The plant cell* 16(5):1327-1339.
61. Jacobs AK, *et al.* (2003) An Arabidopsis callose synthase, GSL5, is required for wound and papillary callose formation. *The Plant Cell* 15(11):2503-2513.
62. Järup L (2003) Hazards of heavy metal contamination. *British medical bulletin* 68(1):167-182.
63. Jung CS, *et al.* (2003) Dynamics of callose deposition during reproductive events in sexual and apomictic Allium species. *한국육종학회/ 학술발표회/ 발표요지* 35(1):71-71.
64. Kawachi M, *et al.* (2009) A mutant strain Arabidopsis thaliana that lacks vacuolar membrane zinc transporter MTP1 revealed the latent tolerance to excessive zinc. *Plant and Cell Physiology* 50(6):1156-1170.
65. Kim I, Hempel FD, Sha K, Pfluger J, & Zambryski PC (2002) Identification of a developmental transition in plasmodesmatal function during embryogenesis in Arabidopsis thaliana. *Development* 129(5):1261-1272.
66. Kim W, Ahn HJ, Chiou T-J, & Ahn JH (2011) The role of the miR399-PHO2 module in the regulation of flowering time in response to different ambient temperatures in Arabidopsis thaliana. *Molecules and cells* 32(1):83-88.
67. Kobayashi Y, *et al.* (2008) Amino acid polymorphisms in strictly conserved domains of a P-type ATPase HMA5 are involved in the mechanism of copper tolerance variation in Arabidopsis. *Plant Physiology* 148(2):969-980.
68. Köhler P & Carr DJ (2006) A somewhat obscure discoverer of plasmodesmata: Eduard Tangl (1848–1905). *The global and the local: the history of science and the cultural integration of Europe. Proceedings of the 2nd ICESHS*:6-9.
69. Koizumi K, Hayashi T, Wu S, & Gallagher KL (2012) The SHORT-ROOT protein acts as a mobile, dose-dependent signal in patterning the ground tissue. *Proceedings of the National Academy of Sciences* 109(32):13010-13015.
70. Konno M, Ooishi M, & Inoue Y (2003) Role of manganese in low-pH-induced root hair formation in Lactuca sativa cv. Grand Rapids seedlings. *Journal of plant research* 116(4):301-307.

71. Kurata T, *et al.* (2005) Cell-to-cell movement of the CAPRICE protein in Arabidopsis root epidermal cell differentiation. *Development* 132(24):5387-5398.
72. Lachaud S & Maurousset L (1996) Occurrence of plasmodesmata between differentiating vessels and other xylem cells in *Sorbus torminalis* L. Crantz and their fate during xylem maturation. *Protoplasma* 191(3):220-226.
73. Lang A (1965) Physiology of flower initiation. *Differenzierung und Entwicklung/Differentiation and Development*, (Springer), pp 1380-1536.
74. Lanquar V, *et al.* (2010) Export of vacuolar manganese by AtNRAMP3 and AtNRAMP4 is required for optimal photosynthesis and growth under manganese deficiency. *Plant physiology* 152(4):1986-1999.
75. Lee J-Y, *et al.* (2011) A plasmodesmata-localized protein mediates crosstalk between cell-to-cell communication and innate immunity in Arabidopsis. *The Plant Cell Online* 23(9):3353-3373.
76. Levy A, Erlanger M, Rosenthal M, & Epel BL (2007) A plasmodesmata-associated β -1, 3-glucanase in Arabidopsis. *The Plant Journal* 49(4):669-682.
77. Levy A, Zheng JY, & Lazarowitz SG (2015) Synaptotagmin SYTA forms ER-plasma membrane junctions that are recruited to plasmodesmata for plant virus movement. *Current Biology* 25(15):2018-2025.
78. Li X, Poon C-s, & Liu PS (2001) Heavy metal contamination of urban soils and street dusts in Hong Kong. *Applied geochemistry* 16(11):1361-1368.
79. Lichten LA & Cousins RJ (2009) Mammalian zinc transporters: nutritional and physiologic regulation. *Annual review of nutrition* 29:153-176.
80. Lin S-I & Chiou T-J (2008) Long-distance movement and differential targeting of microRNA399s. *Plant signaling & behavior* 3(9):730-732.
81. Liu D, Jiang W, Wang W, Zhao F, & Lu C (1994) Effects of lead on root growth, cell division, and nucleolus of *Allium cepa*. *Environmental Pollution* 86(1):1-4.
82. Lucas WJ, Bouché-Pillon S, Jackson DP, & Nguyen L (1995) Selective trafficking of KNOTTED1 homeodomain protein and its mRNA through plasmodesmata. *Science* 270(5244):1980.
83. Lux A, Martinka M, Vaculík M, & White PJ (2011) Root responses to cadmium in the rhizosphere: a review. *Journal of Experimental Botany* 62(1):21-37.
84. Maksimović I, Kastori R, Krstić L, & Luković J (2007) Steady presence of cadmium and nickel affects root anatomy, accumulation and distribution of essential ions in maize seedlings. *Biologia Plantarum* 51(3):589-592.
85. Martell EA (1974) Radioactivity of tobacco trichomes and insoluble cigarette smoke particles. *Nature* 249(5454):215-217.
86. Mira H, Martínez-García F, & Peñarrubia L (2001) Evidence for the plant-specific intercellular transport of the Arabidopsis copper chaperone CCH. *The Plant Journal* 25(5):521-528.
87. Monaghan J & Zipfel C (2012) Plant pattern recognition receptor complexes at the plasma membrane. *Current opinion in plant biology* 15(4):349-357.
88. Mukherjee I, Campbell NH, Ash JS, & Connolly EL (2006) Expression profiling of the Arabidopsis ferric chelate reductase (FRO) gene family reveals differential regulation by iron and copper. *Planta* 223(6):1178-1190.
89. Müller J, *et al.* (2015) Iron-Dependent Callose Deposition Adjusts Root Meristem Maintenance to Phosphate Availability. *Developmental cell* 33(2):216-230.
90. Mwegoha W & Kihampa C (2010) Heavy metal contamination in agricultural soils and water in Dar es Salaam city, Tanzania. *African Journal of Environmental Science and Technology* 4(11):763-769.

91. Nagajyoti P, Lee K, & Sreekanth T (2010) Heavy metals, occurrence and toxicity for plants: a review. *Environmental Chemistry Letters* 8(3):199-216.
92. Nicolas WJ, *et al.* (2017) Architecture and permeability of post-cytokinesis plasmodesmata lacking cytoplasmic sleeves. *Nature plants* 3:17082.
93. Nishikawa S-i, Zinkl GM, Swanson RJ, Maruyama D, & Preuss D (2005) Callose (β -1, 3 glucan) is essential for Arabidopsis pollen wall patterning, but not tube growth. *BMC Plant Biology* 5(1):22.
94. Oparka K & Prior D (1992) Direct evidence for pressure-generated closure of plasmodesmata. *The Plant Journal* 2(5):741-750.
95. Oparka KJ, *et al.* (1999) Simple, but not branched, plasmodesmata allow the nonspecific trafficking of proteins in developing tobacco leaves. *Cell* 97(6):743-754.
96. Ortega-Villasante C, Hernández LE, Rellán-Álvarez R, Del Campo FF, & Carpena-Ruiz RO (2007) Rapid alteration of cellular redox homeostasis upon exposure to cadmium and mercury in alfalfa seedlings. *New Phytologist* 176(1):96-107.
97. Ouzounidou G (1994) Copper-induced changes on growth, metal content and photosynthetic function of *Alyssum montanum* L. plants. *Environmental and Experimental Botany* 34(2):165-172.
98. Palevitz B & Hepler P (1985) Changes in dye coupling of stomatal cells of *Allium* and *Commelina* demonstrated by microinjection of Lucifer yellow. *Planta* 164(4):473-479.
99. Pant BD, Buhtz A, Kehr J, & Scheible WR (2008) MicroRNA399 is a long-distance signal for the regulation of plant phosphate homeostasis. *The Plant Journal* 53(5):731-738.
100. Patra M, Bhowmik N, Bandyopadhyay B, & Sharma A (2004) Comparison of mercury, lead and arsenic with respect to genotoxic effects on plant systems and the development of genetic tolerance. *Environmental and Experimental Botany* 52(3):199-223.
101. Pendle A & Benitez-Alfonso Y (2015) Immunofluorescence Detection of Callose Deposition Around Plasmodesmata Sites. *Plasmodesmata: Methods and Protocols*:95-104.
102. Phang C, Leung DW, Taylor HH, & Burritt DJ (2011) Correlation of growth inhibition with accumulation of Pb in cell wall and changes in response to oxidative stress in *Arabidopsis thaliana* seedlings. *Plant growth regulation* 64(1):17-25.
103. Pich A, Scholz G, & Stephan UW (1994) Iron-dependent changes of heavy metals, nicotianamine, and citrate in different plant organs and in the xylem exudate of two tomato genotypes. Nicotianamine as possible copper translocator. *Plant and Soil* 165(2):189-196.
104. Prinz WA (2014) Bridging the gap: membrane contact sites in signaling, metabolism, and organelle dynamics. *J Cell Biol* 205(6):759-769.
105. Pumplun N & Voinnet O (2013) RNA silencing suppression by plant pathogens: defence, counter-defence and counter-counter-defence. *Nature Reviews. Microbiology* 11(11):745.
106. Punshon T, Guerinot ML, & Lanzirotti A (2009) Using synchrotron X-ray fluorescence microprobes in the study of metal homeostasis in plants. *Annals of Botany* 103(5):665-672.

107. Qi Y & Katagiri F (2012) Membrane microdomain may be a platform for immune signaling. *Plant signaling & behavior* 7(4):454-456.
108. Reyt G, Boudouf S, Boucherez J, Gaymard F, & Briat J-F (2014) Iron and ferritin dependent ROS distribution impact Arabidopsis root system architecture. *Molecular plant*.
109. Rim Y, *et al.* (2011) Analysis of Arabidopsis transcription factor families revealed extensive capacity for cell-to-cell movement as well as discrete trafficking patterns. *Molecules and cells* 32(6):519-526.
110. Rinne PL, Kaikuranta PM, & Van Der Schoot C (2001) The shoot apical meristem restores its symplasmic organization during chilling-induced release from dormancy. *The Plant Journal* 26(3):249-264.
111. Roberts AG, *et al.* (1997) Phloem unloading in sink leaves of *Nicotiana benthamiana*: comparison of a fluorescent solute with a fluorescent virus. *The Plant Cell Online* 9(8):1381-1396.
112. Roy J, Caldwell MM, & Pearce RP (2012) *Exploitation of environmental heterogeneity by plants: ecophysiological processes above-and belowground* (Academic Press).
113. Saatian B (2016) GLUCAN SYNTHASE-LIKE 8: A Key Player in Early Seedling Development in Arabidopsis.
114. Salt DE, Prince RC, Pickering IJ, & Raskin I (1995) Mechanisms of cadmium mobility and accumulation in Indian mustard. *Plant Physiology* 109(4):1427-1433.
115. Sancenón V, *et al.* (2004) The Arabidopsis copper transporter COPT1 functions in root elongation and pollen development. *Journal of Biological Chemistry* 279(15):15348-15355.
116. Savage N, *et al.* (2013) Positional signaling and expression of ENHANCER OF TRY AND CPC1 are tuned to increase root hair density in response to phosphate deficiency in Arabidopsis thaliana. *PLoS One* 8(10):e75452.
117. Schönknecht G, Brown J, & Verchot-Lubicz J (2008) Plasmodesmata transport of GFP alone or fused to potato virus X TGBp1 is diffusion driven. *Protoplasma* 232(3-4):143-152.
118. Schulz A (1995) Plasmodesmal widening accompanies the short-term increase in symplasmic phloem unloading in pea root tips under osmotic stress. *Protoplasma* 188(1):22-37.
119. Schützendubel A & Polle A (2002) Plant responses to abiotic stresses: heavy metal-induced oxidative stress and protection by mycorrhization. *Journal of experimental botany* 53(372):1351-1365.
120. Senden M, Van der Meer A, Verburg T, & Wolterbeek HT (1995) Citric acid in tomato plant roots and its effect on cadmium uptake and distribution. *Plant and Soil* 171(2):333-339.
121. Seregin I, Kozhevnikova A, Kazyumina E, & Ivanov V (2003) Nickel toxicity and distribution in maize roots. *Russian Journal of Plant Physiology* 50(5):711-717.
122. Sharma RK, Agrawal M, & Marshall F (2007) Heavy metal contamination of soil and vegetables in suburban areas of Varanasi, India. *Ecotoxicology and environmental safety* 66(2):258-266.
123. Shepherd V, Orlovich D, & Ashford A (1993) Cell-to-cell transport via motile tubules in growing hyphae of a fungus. *Journal of cell science* 105(4):1173-1178.
124. Shimotohno A, *et al.* (2015) Mathematical Modeling and Experimental Validation of the Spatial Distribution of Boron in the Root of Arabidopsis thaliana Identify

- High Boron Accumulation in the Tip and Predict a Distinct Root Tip Uptake Function. *Plant and Cell Physiology*:pcv016.
125. Simpson C, Thomas C, Findlay K, Bayer E, & Maule AJ (2009) An Arabidopsis GPI-anchor plasmodesmal neck protein with callose binding activity and potential to regulate cell-to-cell trafficking. *The Plant Cell* 21(2):581-594.
 126. Sinclair SA, Sherson SM, Jarvis R, Camakaris J, & Cobbett CS (2007) The use of the zinc-fluorophore, Zinpyr-1, in the study of zinc homeostasis in Arabidopsis roots. *New Phytologist* 174(1):39-45.
 127. Sivaguru M, *et al.* (2000) Aluminum-induced 1 \rightarrow 3- β -d-glucan inhibits cell-to-cell trafficking of molecules through plasmodesmata. A new mechanism of aluminum toxicity in plants. *Plant physiology* 124(3):991-1006.
 128. Steinhorst L & Kudla J (2013) Calcium and reactive oxygen species rule the waves of signaling. *Plant physiology* 163(2):471-485.
 129. Steudle E (1994) Water transport across roots. *Plant and Soil* 167(1):79-90.
 130. Stonebloom S, *et al.* (2012) Redox states of plastids and mitochondria differentially regulate intercellular transport via plasmodesmata. *Plant physiology* 158(1):190-199.
 131. Stonebloom S, *et al.* (2009) Loss of the plant DEAD-box protein ISE1 leads to defective mitochondria and increased cell-to-cell transport via plasmodesmata. *Proceedings of the National Academy of Sciences* 106(40):17229-17234.
 132. Su S, *et al.* (2010) Cucumber mosaic virus movement protein severs actin filaments to increase the plasmodesmal size exclusion limit in tobacco. *The Plant Cell* 22(4):1373-1387.
 133. Suzuki N (2005) Alleviation by calcium of cadmium-induced root growth inhibition in Arabidopsis seedlings. *Plant Biotechnology* 22(1):19-25.
 134. Terry B & Robards A (1987) Hydrodynamic radius alone governs the mobility of molecules through plasmodesmata. *Planta* 171(2):145-157.
 135. Thomine S, Lelièvre F, Debarbieux E, Schroeder JI, & Barbier-Brygoo H (2003) AtNRAMP3, a multispecific vacuolar metal transporter involved in plant responses to iron deficiency. *The Plant Journal* 34(5):685-695.
 136. Thomine S, Wang R, Ward JM, Crawford NM, & Schroeder JI (2000) Cadmium and iron transport by members of a plant metal transporter family in Arabidopsis with homology to Nramp genes. *Proceedings of the National Academy of Sciences* 97(9):4991-4996.
 137. Tsukagoshi H, Busch W, & Benfey PN (2010) Transcriptional regulation of ROS controls transition from proliferation to differentiation in the root. *Cell* 143(4):606-616.
 138. Tucker E (1987) Cytoplasmic streaming does not drive intercellular passage in staminal hairs of *Setcreasea purpurea*. *Protoplasma* 137(2):140-144.
 139. Vatén A, *et al.* (2011) Callose biosynthesis regulates symplastic trafficking during root development. *Developmental cell* 21(6):1144-1155.
 140. Verma S & Dubey R (2003) Lead toxicity induces lipid peroxidation and alters the activities of antioxidant enzymes in growing rice plants. *Plant Science* 164(4):645-655.
 141. Vert G, Briat JF, & Curie C (2001) Arabidopsis IRT2 gene encodes a root-periphery iron transporter. *The Plant Journal* 26(2):181-189.
 142. Wang K, Zhou B, Kuo Y-M, Zemansky J, & Gitschier J (2002) A novel member of a zinc transporter family is defective in acrodermatitis enteropathica. *The American Journal of Human Genetics* 71(1):66-73.

143. Wei B & Yang L (2010) A review of heavy metal contaminations in urban soils, urban road dusts and agricultural soils from China. *Microchemical Journal* 94(2):99-107.
144. Willmann R, *et al.* (2011) Arabidopsis lysin-motif proteins LYM1 LYM3 CERK1 mediate bacterial peptidoglycan sensing and immunity to bacterial infection. *Proceedings of the National Academy of Sciences* 108(49):19824-19829.
145. Wolf S, LUCAS WJ, DEOM CM, & BEACHY RN (1989) Movement protein of tobacco mosaic virus modifies plasmodesmatal size exclusion limit. *Science* 246(4928):377-379.
146. Wong CKE & Cobbett CS (2009) HMA P-type ATPases are the major mechanism for root-to-shoot Cd translocation in Arabidopsis thaliana. *New phytologist* 181(1):71-78.
147. Wong M & Bradshaw A (1982) A comparison of the toxicity of heavy metals, using root elongation of rye grass, Lolium perenne. *New Phytologist* 91(2):255-261.
148. Wu Q-S & Xia R-X (2006) Arbuscular mycorrhizal fungi influence growth, osmotic adjustment and photosynthesis of citrus under well-watered and water stress conditions. *Journal of plant physiology* 163(4):417-425.
149. Wu S & Gallagher KL (2013) Intact microtubules are required for the intercellular movement of the SHORT-ROOT transcription factor. *The Plant Journal* 74(1):148-159.
150. Wu S & Gallagher KL (2014) The movement of the non-cell-autonomous transcription factor, SHORT-ROOT relies on the endomembrane system. *The Plant Journal* 80(3):396-409.
151. Wu S, *et al.* (2016) Symplastic signaling instructs cell division, cell expansion, and cell polarity in the ground tissue of Arabidopsis thaliana roots. *Proceedings of the National Academy of Sciences*:201610358.
152. Wu X, *et al.* (2003) Modes of intercellular transcription factor movement in the Arabidopsis apex. *Development* 130(16):3735-3745.
153. Xu XM, *et al.* (2011) Chaperonins facilitate KNOTTED1 cell-to-cell trafficking and stem cell function. *Science* 333(6046):1141-1144.
154. Yamasaki H, Hayashi M, Fukazawa M, Kobayashi Y, & Shikanai T (2009) SQUAMOSA promoter binding protein-like7 is a central regulator for copper homeostasis in Arabidopsis. *The Plant Cell* 21(1):347-361.
155. Yang H-Q & Jie Y-L (2005) Uptake and transport of calcium in plants. *Zhi wu sheng li yu fen zi sheng wu xue xue bao= Journal of plant physiology and molecular biology* 31(3):227-234.
156. Zambryski P (2004) Cell-to-cell transport of proteins and fluorescent tracers via plasmodesmata during plant development. *The Journal of cell biology* 164(2):165-168.
157. Zavaliev R & Epel BL (2015) Imaging Callose at Plasmodesmata Using Aniline Blue: Quantitative Confocal Microscopy. *Plasmodesmata*, (Springer), pp 105-119.
158. Zeevaart JA (1976) Physiology of flower formation. *Annual Review of Plant Physiology* 27(1):321-348.
159. Zhai Z, *et al.* (2014) OPT3 is a phloem-specific iron transporter that is essential for systemic iron signaling and redistribution of iron and cadmium in Arabidopsis. *The Plant Cell Online* 26(5):2249-2264.

160. Zhang H, *et al.* (2015) Transgenic *Arabidopsis thaliana* plants expressing a β -1, 3-glucanase from sweet sorghum (*Sorghum bicolor* L.) show reduced callose deposition and increased tolerance to aluminium toxicity. *Plant, cell & environment* 38(6):1178-1188.
161. Zhang H, *et al.* (2009) A soil bacterium regulates plant acquisition of iron via deficiency-inducible mechanisms. *The Plant Journal* 58(4):568-577.
162. Zhang H, Xia Y, Wang G, & Shen Z (2008) Excess copper induces accumulation of hydrogen peroxide and increases lipid peroxidation and total activity of copper–zinc superoxide dismutase in roots of *Elsholtzia haichowensis*. *Planta* 227(2):465-475.
163. Zhang Y & Yang X (1994) The toxic effects of cadmium on cell division and chromosomal morphology of *Hordeum vulgare*. *Mutation Research/Environmental Mutagenesis and Related Subjects* 312(2):121-126.